Thermodynamic perturbation theory for multipolar and ionic liquids

by B. LARSEN†

Department of Chemistry, University of Bergen,
N–5014 Bergen-Univ., Norway

J. C. RASAIAH‡

Department of Chemistry, Royal Holloway College, (London University)
and
Physical Chemistry Laboratory, Oxford University, Oxford

and G. STELL

Department of Mechanics, State University of New York,
Stony Brook, New York 11794

We extend earlier work of ours on the use of Padé approximants in the theory of multipolar and ionic potentials. The new features are (i) extension of our work to mixed multipole terms and inclusion of polarizability, (ii) formulation and implementation of a systematic means of getting analytic approximations for all the two-body and three-body terms appearing in the theory, (iii) assessment of the ionic Padé results in the low-concentration region important in ionic-solution applications, (iv) use of the Padé in a mixed perturbation theory of improved accuracy in that low-concentration regime. The results of (iii) and (iv) are used to study the remarkable low-density charged-sphere critical point recently discovered by Stell, Wu, and Larsen.

---

1. INTRODUCTION

This work is part of a continuing study concerned with thermodynamic perturbation theories for polar systems [1–3]. In a previous paper [1] (hereafter referred to as I) we considered a system of axially symmetric molecules with a point-quadrupole located at each molecular centre. In the present paper we extend that work to include polarizable molecules with *both* point-dipoles *and* point-quadrupoles located at each molecular centre, and simple electrolytes with varying charges. We largely restrict ourselves to molecules with spherical cores but treat both ionic and neutral systems together because the terms which appear in the perturbation series for each system have certain features in common that allow their evaluation by very similar analytical and numerical techniques. By discussing them in the same paper we also hope to draw attention to the fact that our work constitutes the basis for a novel and comprehensive treatment of an ionic solution viewed as a mixture of ions and polarizable polar molecules.

† Present address: Department of Mechanical Engineering, State University of New York, Stony Brook, N.Y. 11794, U.S.A.

‡ On leave of absence from the Department of Chemistry, University of Maine, Orono, Maine 04473, U.S.A.

As in I, the perturbation theory consists, in the present case, of treating the polar interactions (including the monopolar ones, i.e. the charges) as a perturbation to the non-polar reference system, via an expansion of f, the Helmholtz free energy per particle, in terms of the parameter λ, which is the strength of the perturbation. In the case of dipolar and multipolar systems this expansion reads

$$f = f^0 + f^{(1)} \lambda + f^{(2)} \lambda^2 + f^{(3)} \lambda^3 + \dots . \tag{1.1}$$

The coefficients $f^{(n)}$ are characteristic of the reference system, and in particular f^0 is its free energy per particle. Apart from $f^{(1)}$ (which is identically zero for the systems upon which we focus), $f^{(n)}$ involves n-body correlation functions of the reference system. As in previous work on molecules with dipoles [2, 3] or quadrupoles [1], we do not go beyond the term of $O(\lambda^3)$ in the theory, but assuming that the series (1.1) is approximately represented by a geometric series, we have followed our previous work in forming a simple Padé approximant which extrapolates the free energies to higher orders in λ. Computer simulation studies on dipolar or quadrupolar systems have shown that this is an accurate method to adopt, even for high values of the perturbation parameter μ (dipole moment) or Θ (quadrupole moment) [4].

The theory above applies most directly to molecules with point-dipoles or point-multipoles embedded in spherically symmetric cores. Although we have considered [1] a hybrid of our own work with Sandler's discussion of the effect of non-spherical cores [5], the accuracy of this last approach has yet to be tested against the 'exact' values obtained from simulation studies. We note however that one such study of N_2 by Weis and Levesque [6] lends strong general support to the hope that important features of such systems can be treated in terms of a judiciously selected equivalent spherically symmetric pair potential. And even without extension to include the effect of non-spherical cores, we believe our own approach provides valuable insight into new features that appear when dipoles and multipoles are present. It has also led to a re-examination of dipolar solids [7] and mixtures of polar fluids [8] by methods that are closely allied to the way in which polar fluids have been treated [1, 2].

Except for a discussion of the terms of $O(\lambda^2)$, our earlier work [1, 3] has been confined to molecules with only a single point-dipole or point-quadrupole. The presence of more than one multipole on a molecule leads additionally to mixed terms in the free energy beginning at $O(\lambda^2)$. We evaluate here the complete set of free energy terms to $O(\lambda^3)$ for hard spheres with point-dipoles and point-quadrupoles. When the molecules are optically isotropic the perturbation theory and Padé technique can be extended to include polarizable molecules as well [4, 9]. McDonald [4] has demonstrated that the contribution from the polarizability is significant in comparison to the contributions arising from permanent dipoles in polarizable Stockmayer molecules corresponding to real HCl molecules with respect to the values of the permanent dipole and the polarizability. Accordingly our own calculations of the phase diagram for HCl-type molecules with point-dipoles and point-quadrupoles include polarizability effects also, but only as far as the dipole-induced dipole terms discussed in McDonald's paper.

In I we proved a theorem which demonstrates that two-body terms of $O(\lambda^{2n+1})$ in the free energy are zero for certain combinations of two multipoles.

In the present work we extend this theorem to include mixed many-body terms to any order of λ. Special examples are given by the application of the theorem to the cases of interest here ; two and three-body terms of $O(\lambda^3)$ arising from dipoles *and* quadrupoles on each molecule. The application of the theorem is, however, not limited to thermodynamic perturbation theory, because the theorem is based on a rather fundamental property of spherical harmonics. This is discussed in § 2 where we are led to a simple but powerful criterion for determining, by inspection, whether a cluster integral of angle-dependent potential energy bonds on N vertices is identically zero. When they are non-zero, angular averaging is followed by spatial integration (which we discuss in § 3) of the two and three-body terms of $O(\lambda^2)$ and $O(\lambda^3)$. The integration of the three-body contribution to $O(\lambda^3)$, the result of which is essentially given as the triple integral $I_{\text{triple}}^{\text{HS}}$, proceeds along the lines introduced by us for triple-quadrupoles [1]. We extrapolate our results for f beyond $O(\lambda^3)$ by using the Padé approximant

$$f^{\text{P}} = f^0 + f_2 \left[1 - \frac{f_3}{f_2} \right]^{-1} \tag{1.2}$$

where f^0 is the free energy of the reference system and f_2 and f_3 are the contributions to f of $O(\lambda^2)$ and of $O(\lambda^3)$, respectively. Polarizable molecules are next considered in the same section by simply adding to f^{P} the free energy contributions due to the polarizabilities. On this basis the liquid–gas co-existence curve for the model system is constructed.

We conclude that the dipole-induced dipole contribution is significant in our model corresponding to real HCl, although we find that it is much less important than in the polarizable Stockmayer model [4], because the permanent quadrupole in HCl also gives a dominant contribution which tends to reduce the relative importance of the polarizability.

Three-body terms similar to those appearing in the perturbation theory of polar fluids also appear in the Stell–Lebowitz [10] (SL) theory of charged particles and in the mode expansion due to Andersen and Chandler [11]. Stell and Wu [12] have in fact used a Padé approximant for symmetrically charged spheres to extend the application of the theory into the molten salt range. Our method of calculating $I_{\text{triple}}^{\text{HS}}$ is, with minor modifications, applicable to the evaluation of the three-body integrals occurring in the SL theory. We find it convenient to discuss this separately in § 4, where we also consider the union of a Padé approximant derived from a truncated Stell–Lebowitz theory with the second ionic virial coefficient B_2 [13]. We refer to this as the SL6(P)$\cup B_2$ theory. It gives the Debye–Hückel limiting law plus B_2 at low values of the perturbation parameter and the Padé approximant, which we call SL6(P), at high values. It is the first theory which has combined these features in a simple way, and it represents a considerable improvement of the SL6(P) in the density and temperature region corresponding to a dilute electrolyte model. We use it here to study the vicinity of the low-density charged-sphere critical point recently discovered by Stell *et al.* [14].

Our success in formulating simple analytic expressions for ionic and multi-polar systems in the liquid-density regime has been facilitated by the remarkable smoothness as functions of ρ of the coefficients in our λ expansions and Padé

approximants in λ.   These coefficients are integrals over pair and triple distribution functions g and g_{123} [e.g. the $I_n{}^{\text{HS}}$ and $I_{\text{triple}}{}^{\text{HS}}$ of equations (3.9) and (3.12)] which for fixed molecular positions change markedly and rapidly as ρ increases.   Yet the integrals are sufficiently slowly and smoothly varying with ρ that they can be well approximated throughout the whole liquid-density range by simple polynomials and Padé approximants in ρ based on the first few terms of their density expansions.

As noted in previous work [3], these integrals, and variants of them, are ubiquitous in liquid-theory perturbation approaches for simple atomic as well as polar and ionic fluids.   In Appendix A we give an accurate and extensive set of approximants for the $I_n{}^{\text{HS}}$ that extends our earlier results for this function while in Appendix B we consider the systematic evaluation of the coefficients J_i in the density expansion of the triple integral $I_{\text{triple}}{}^{\text{HS}}(x)$, where $x = \rho a^3$ is a reduced density and a is the molecular diameter

$$I_{\text{triple}}{}^{\text{HS}}(x) = J_0 + J_1 x + J_2 x^2 + J_3 x^3 + \dots . \qquad (1.3)$$

This integral appears in the three-body term of $O(\lambda^3)$, and also in the dipole-induced dipole terms of $O(\alpha\mu^4)$ and $O(\alpha^2\mu^2)$ where α is the polarizability [4] and μ the dipole-moment strength.   In the case of a hard-sphere reference system the individual J_0 coefficients due to three-body interactions between permanent dipoles and/or multipoles are also related to the high-temperature non-additive contributions to the third virial coefficient arising from dispersion forces.   These are in fact given by $\beta Z(ijk) J_0\{ijk\}/3$ where $\beta = 1/k_B T$ and the set $\{ijk\}$ characterizes the type of three-body dispersion force (triple-dipole, etc.). The interaction coefficients $Z(ijk)$ are those discussed by Bell [15] and others [16].   Another application of the technique occurs in the calculation of effective pair potentials from non-additive dispersion and induction forces [17, 18]. Finally, all of our work here can be directly extended to mixtures of dipolar and quadrupolar fluids.

. Two important papers that extend the Padé technique of I and complement this work have recently appeared.[19], one by Flytzani-Stephanopoulos *et al.* and one by Patey and Valleau.   The first reveals the sensitivity of the phase boundaries in mixtures to the strengths and relative magnitudes of the dipole and quadrupole moments of the component molecules (this was already apparent in the single-component case from the results of reference [3]).   Both further suggest that the presence of dipolar and quadrupolar forces are sufficient to account for a good deal of the variety in the qualitatively different sorts of phase surfaces experimentally found for molecular fluids but not found either experimentally or theoretically for fluids of monatomic molecules.   We anticipate that our methods of analytically approximating and evaluating the doublet and triplet integrals treated herein will prove to be of special value in facilitating future mixture studies that would be prohibitively difficult to do accurately without such computational methods at hand.

Because of their wide applicability, we regard the mathematical developments of our Appendices as constituting a central accomplishment of this paper. We refrain from further discussion of most of the applications and extensions that we have noted in order to keep the paper a manageable length.   Some of them are so immediate as to require no further elaboration ; the rest we hope to take up in due course.

2. MANY-BODY INTERACTIONS FOR SPHERICALLY SYMMETRIC MOLECULES WITH POINT-DIPOLES AND POINT-MULTIPOLES

The angularly averaged two-body potential of $O(\lambda^n)$ may be obtained from the expression

$$\bar{u} = -\frac{1}{\beta}\ln\,\langle\exp\,[-\beta\sum_k\lambda_k w_{l_i l_j}(\mathbf{x}_i,\mathbf{x}_j)]\rangle_\omega, \qquad (2.1)$$

where the index k represents the pair of multipoles (l_i, l_j) on molecules i and j which are assumed to be spherically symmetric. Their energy of interaction is $\lambda_k w_{l_i l_j}(\mathbf{x}_i, \mathbf{x}_j)$ where $\mathbf{x}_q \equiv (\mathbf{r}_q, \omega_q)$ defines the position $(\mathbf{r}_q)$ and orientation (ω_q) of the qth molecule.

In (2.1), $\langle (\quad) \rangle_\omega$ denotes $1/(4\pi)^2\int(\quad)\,d\omega_1\,d\omega_2$ and $\beta=(k_B T)^{-1}$, where k_B is Boltzmann's constant and T is the absolute temperature. Since $\langle w_{l_1 l_2}\rangle_\omega=0$ for point-dipoles and point-multipoles, the term of $O(\lambda^3)$ in (2.1) comes from $-(\beta^2/3\,!)\langle[\sum_k\lambda_k w_{l_i l_j}(\mathbf{x}_1,\mathbf{x}_2)]^3\rangle_\omega$. Our notation here is the same as that used in I. In particular we wish to recall that l_i (or l_j) is 1, 2 or 3 according to whether a point-dipole, point-quadrupole or point-octupole resides at i (or j).

In what follows it is convenient to characterize in greater detail the interactions between two vertices i and j in a cluster integral of potential energy bonds. Such integrals (or graphs representing them) appear in the perturbation theory of polar fluids [1]. We will use three indices (ij, p) to characterize a particular bond between i and j. The index p ranges over the number n_{ij} of bonds between i and j, and instead of l_i we will write $l_{ij,p}$ to denote the multipole on vertex i interacting along the pth bond with vertex j. The potential energy of interaction between two molecules at i and j, $\lambda w(\mathbf{x}_i, \mathbf{x}_j)$, can be expressed as an expansion in spherical harmonics through the equations

$$\lambda w(\mathbf{x}_i, \mathbf{x}_j) = \sum_k \lambda_k w_{l_{ij,p}\,l_{ji,p}}(\mathbf{x}_i, \mathbf{x}_j), \qquad (2.2)$$

where k represents the pair of multipoles $(l_{ij,p}, l_{ji,p})$, $\sum_k$ is equivalent to $\sum_{l_{ij,p}}\sum_{l_{ji,p}}$ and

$$\lambda_k w_{l_{ij,p}\,l_{ji,p}}(\mathbf{x}_i, \mathbf{x}_j) = 4\pi\sum_{m_{ij,p}} X^{l_{ij,p}\,l_{ji,p}\,m_{ij,p}}(r_{ij})$$
$$\times S_{l_{ij,p}\,m_{ij,p}}(\theta_i^{ij}, \phi_i^{ij})S_{l_{ji,p}\,m_{ij,p}}(\theta_j^{ji}, \phi_j^{ji}). \qquad (2.3)$$

In (2.3) $X^{l_{ij,p}\,l_{ji,p}\,m_{ij,p}}(r_{ij})$ (denoted in our earlier work as $X^{l l' m}(r)$) is the interaction coefficient between the pair of multipoles $(l_{ij,p}, l_{ji,p})$ on the molecules at i and j, respectively, at separation r_{ij}. The integer $m_{ij,p}$ extends from $-\min(l_{ij,p}, l_{ji,p})$ to $+\min(l_{ij,p}, l_{ji,p})$, and the pairs of angles $(\theta_i^{ij}, \phi_i^{ij})$ and $(\theta_j^{ji}, \phi_j^{ji})$ determine the orientations of the multipoles at i and j.

A general contribution to the two-body term of $O(\lambda^3)$ in the free energy (see (2.1)) may be represented by

$$\left\langle\prod_{p=1}^{3}\lambda_k w_{l_{12,p}\,l_{21,p}}(\mathbf{x}_1, \mathbf{x}_2)\right\rangle_\omega = 4\pi\sum_{m_{12,1}}\sum_{m_{12,2}}\sum_{m_{12,3}}\prod_{p=1}^{3}X^{l_{12,p}\,l_{21,p}\,m_{21,p}}(r_{12})$$
$$\times C_{\{m_{12,p}\}}^{\{l_{12,p}\}}C_{\{m_{12,p}\}}^{\{l_{21,p}\}}, \qquad (2.4)$$

where $\{l_{12,p}\}$ represents the set $(l_{12,1}, l_{12,2}, l_{12,3})$, and a similar explanation holds

for $\{l_{21\ p}\}$ and $\{m_{12,p}\}$. Then in (2.4),

$$C_{\{m_{12,p}\}}^{\{l_{12,p}\}} = 2\pi\delta\left(\sum_{p=1}^{3} m_{12,p}\right) K\left[1 + (-1)^{\sum_{p=1}^{3} l_{12,p} + |m_{12,p}|}\right]$$

$$\times \int_0^1 \prod_{p=1}^{3} P_{l_{12,p}}^{|m_{12,p}|}(x)\, dx \qquad (2.5)$$

with an analogous expression for $C_{\{m_{12,p}\}}^{\{l_{21,p}\}}$. In (2.5), K is a normalization constant, $P_{l_{12,p}}^{|m_{12,p}|}(x)$ the associated Legendre function and $\delta(\ )$ is the Kronecker delta. In arriving at (2.5), the parity of the associated Legendre functions [1] has been used. Since $\sum_{p=1}^{3} m_{12,p} = 0$ implies that $\sum_{p=1}^{3} |m_{12,p}|$ is even, it follows that $C_{\{m_{12,p}\}}^{\{l_{12,p}\}}$ is zero if $\sum_{p=1}^{3} l_{12,p}$ is odd. An obvious extension of this result is that if there are n_{12} bonds between two vertices, the corresponding $C_{\{m_{12,p}\}}^{\{l_{12,p}\}}$ is zero if $\sum_{p=1}^{n_{12}} l_{12,p}$ is odd.

The above result can also be generalized to apply to many-body interactions. The sum of all irreducible graphs of potential energy bonds between N vertices which contribute a term of $O(\lambda^n)$ to the free energy is

$$\bar{u}_N^{(n)}(\mathbf{r}_1, \mathbf{r}_2, \ldots, \mathbf{r}_N) = \frac{\lambda^n}{n!} \sum_{n_{12}+n_{13}+\ldots=n} \langle w(\mathbf{x}_1, \mathbf{x}_2)^{n_{12}}\, w(\mathbf{x}_1, \mathbf{x}_3)^{n_{13}}\ldots$$

$$\times w(\mathbf{x}_1, \mathbf{x}_N)^{n_{1N}}\ldots w(\mathbf{x}_2, \mathbf{x}_3)^{n_{23}}\ldots w(\mathbf{x}_{N-1}, \mathbf{x}_N)^{n_{N-1,N}}\rangle_{\{\omega\}}. \qquad (2.6)$$

In (2.6) $\bar{u}_N^{(n)}(\mathbf{r}_1, \mathbf{r}_2, \ldots, \mathbf{r}_N)$ is an angularly averaged N-body potential and

$$\langle\langle\ \rangle\rangle_{\{\omega\}} = \frac{1}{(4\pi)^N} \int \ldots \int (\ )\, d\omega_1\, d\omega_2 \ldots d\omega_N. \qquad (2.7)$$

Since $\lambda w(\mathbf{x}_i, \mathbf{x}_j)$ can be written as an expansion in spherical harmonics (see (2.2) and (2.3)), the integral in (2.6) is factorizable. It follows that if the angular integral over any one of the vertices is zero, the contribution of that term (or graph) to $\bar{u}_N^{(n)}(\mathbf{r}_1, \mathbf{r}_2, \ldots, \mathbf{r}_N)$ is also zero.

The angular integral over the ith vertex of a term in the sum (2.6) has the form

$$\int \prod_{\substack{j=1 \\ j\neq i}}^{N} \prod_{p=1}^{n_{ij}} S_{l_{ij,p}\, m_{ij,p}}(\theta_i^{ij}, \phi_i^{ij})\, d\omega_i. \qquad (2.8)$$

To do this integral, all angles $(\theta_i^{ij}, \phi_i^{ij})$ at i are referred to the same axis, which is taken arbitrarily to be the $(i1)$ axis (assuming without prejudice that $i \neq 1$). The spherical harmonics referring to the (ij) axis can be written as linear combinations of the spherical harmonics with respect to the $(i1)$ axis, so that

$$S_{l_{ij,p}\, m_{ij,p}}(\theta_i^{ij}, \phi_i^{ij}) = \sum_{m'_{ij,p} = -l_{ij,p}}^{l_{ij,p}} D_{m'_{ij,p}\, m_{ij,p}}^{l_{ij,p}} S_{l_{ij,p}\, m'_{ij,p}}(\theta_i^{i1}, \phi_i^{i1}), \qquad (2.9)$$

where the coefficients $D_{m'_{ij,p}\, m_{ij,p}}^{l_{ij,p}}$ are constants for a fixed set of vertices i, j and 1. By introducing (2.9) in (2.8), the integral may be expanded as the sum

of products of spherical harmonics referring to the same ($i1$) axis. Since each term in this sum is characterized by the same set of $l_{ij,p}$'s, all terms will be zero after integration if one term can be shown to be zero due to some condition on the set $\{l_{ij,p}\}$ associated with the vertex i. An arbitrary term, when (2.9) and (2.8) are combined, has the form

$$\int \prod_{\substack{j=1 \\ j \neq i}}^{N} \prod_{p=1}^{n_{ij}} S_{l_{ij,p}\, m_{ij,p}} \cdot (\theta_i^{i1}, \phi_i^{i1})\, d\omega_i. \tag{2.10}$$

Using the same argument as for the two-body term of $O(\lambda^3)$, one finds that the above integral is zero if

$$\sum_{\substack{j=1 \\ j \neq i}}^{N} \sum_{p=1}^{n_{ij}} l_{ij,p} \text{ is odd.} \tag{2.11}$$

This implies that *an irreducible cluster diagram contributing to $\bar{u}_N^{(n)}(\mathbf{r}_1, \mathbf{r}_2, ..., \mathbf{r}_N)$ is zero if (2.11) is true for any vertex i ($1 \leqslant i \leqslant N$) in that diagram.* A corollary to this is that, since $\exp(x) \geqslant 1+x$, the corresponding irreducible diagram of Mayer f-bonds is always greater than or equal to zero if the diagram containing only potential bonds is zero.

We will illustrate the general result for potential bonds with two examples that are relevant to the calculations which follow in §§ 3 and 4. Consider the contributions of $O(\lambda^3)$ for a system in which each molecule has a dipole moment and a quadrupole moment. Then representing a dipole–dipole bond by O——O, a dipole–quadrupole bond by O———--O, a quadrupole–dipole bond by O-- ——O, and a quadrupole–quadrupole bond by O- - - - -O, the two-body term of $O(\lambda^3)$ is

$$\bar{u}_2^{(3)}(r_1, r_2) = \frac{1}{3!} \; (\; \ominus + 2 \, \text{⟨⋯⟩} + \text{⟨⋯⟩}$$

$$+ 6 \, \text{⟨⋯⟩} + 3 \, \text{(⋯)} + 6 \, \text{⟨⋯⟩} + 3 \, \text{⟨⋯⟩}$$

$$+ 6 \, \text{⟨⋯⟩} + 6 \, \text{⟨⋯⟩} + 6 \, \text{⟨⋯⟩}$$

$$+ 6 \, \text{⟨⋯⟩} + 12 \, \text{⟨⋯⟩} + 6 \, \text{⟨⋯⟩} \;) \tag{2.12}$$

According to the theorem, all diagrams in (2.12) with $\twoheadleftarrow$ or $\twoheadleftarrow$ vertices are zero, which leaves us with
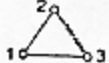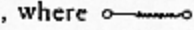
$$\bar{u}_2^{(3)}(\mathbf{r}_1, \mathbf{r}_2) = \frac{1}{3!} \; (\text{⟨⋯⟩} + 3 \, \text{⟨⋯⟩} + 6 \, \text{⟨⋯⟩} + 6 \, \text{⟨⋯⟩} \;) \tag{2.13}$$

Similarly for the three-body term of $O(\lambda^3)$, we find that

$$\bar{u}_3^{(3)}(\mathbf{r}_1, \mathbf{r}_2, \mathbf{r}_3) = \frac{1}{3!} \; (\; \triangle + 3 \, \triangle + 3 \, \triangle + \triangle \;) \tag{2.14}$$

after excluding all diagrams containing at least one $\twoheadleftarrow$ vertex. It is immediately obvious from (2.14) that a vertex in the three-body terms may be associated with either a dipole or a quadrupole; hence the terms as they appear

from left to right in (2.14) are characterized as triple–dipole (TD), dipole–dipole–quadrupole (DDQ), dipole–quadrupole–quadrupole (DQQ) and triple–quadrupole (TQ). It is clear from the analysis above that such an association between vertex and multipole (or dipole) is not always possible, as one can see for the two-body interactions of $O(\lambda^3)$ in (2.13). The special features of the three-body terms in (2.14) would be lost if an octupole ($l_{ij,p}=3$) were also present at each molecule; according to our theorem, non-zero diagrams of the

type , where o——o represent a dipole–octupole bond, would then

appear. One sees now that vertex 3 can no longer be associated with a unique dipole or multipole.

3. Calculations for polarizable hard spheres with point-dipoles and point-quadrupoles

If we recall that $l_{ij,p}$ equals 1 for a dipole and 2 for a quadrupole, the two-body term of $O(\lambda^3)$ given in (2.13) can be written as

$$\bar{u}_2^{(3)}(\mathbf{r}_1, \mathbf{r}_2) = \frac{1}{3!}\left[\Theta^6\langle w_{22}^3\rangle_\omega + 3\mu^4\,\Theta^2\langle w_{11}^2\,w_{22}\rangle_\omega + 6\mu^2\,\Theta^4\langle w_{12}^2\,w_{22}\rangle_\omega\right.$$
$$\left. + 6\mu^4\,\Theta^2\langle w_{11}w_{12}w_{21}\rangle_\omega\right]. \quad (3.1)$$

Of these we have evaluated only the first in I :

$$\langle w_{22}^3\rangle_\omega = \frac{432}{245}\,r^{-15}. \quad (3.2)$$

By using the same method to calculate the other angular averages we find that

$$\langle w_{11}^2\,w_{22}\rangle_\omega = \frac{24}{25}\,r^{-11}, \quad (3.3)$$

$$\langle w_{12}^2\,w_{22}\rangle_\omega = \frac{24}{35}\,r^{-13} \quad (3.4)$$

and

$$\langle w_{11}w_{12}w_{21}\rangle_\omega = \frac{8}{25}\,r^{-11}. \quad (3.5)$$

The two-body term of $O(\lambda^3)$ in the free energy is hence

$$f_{3.2} = \frac{\rho}{2}\,\beta^2\int g_{12}^0(r)\left[\frac{4}{5}\frac{\mu^4\,\Theta^2}{r^{11}} + \frac{24}{35}\frac{\mu^2\,\Theta^4}{r^{13}} + \frac{72}{245}\frac{\Theta^6}{r^{15}}\right]dr, \quad (3.6)$$

where $g_{12}^0(r)$ is the radial distribution function for the reference system. Assuming that these are hard spheres, of diameter a, it is convenient to introduce the reduced variables

$$x = \rho a^3, \quad y = r/a, \quad \mu^{*2} = \mu^2/k_B Ta^3, \quad \text{and} \quad \Theta^{*2} = \Theta^2/k_B Ta^5, \quad (3.7)$$

and rewrite (3.6) as

$$\beta f_{3.2} = x\left[\frac{2\mu^{*4}\,\Theta^{*2}}{5}\,I_{11}^{HS}(x) + \frac{12\mu^{*2}\,\Theta^{*4}}{35}\,I_{13}^{HS}(x) + \frac{36\Theta^{*6}}{245}\,I_{15}^{HS}(x)\right]. \quad (3.8)$$

Here we have used

$$I_n^{HS}(x) \equiv 4\pi \int_0^\infty g^{HS}(x, y) y^{2-n} \, dy, \qquad (3.9)$$

and $g^{HS}(x, y)$ is the hard-sphere radial distribution function. We have arrived at an approximation for (3.9) by expanding $g^{HS}(x, y)$ in a power series in the reduced density (x) and integrating term by term up to $O(x^3)$. This was improved by fitting the coefficients of two additional powers of x to obtain agreement with a numerical computation of $I_n^{HS}(x)$ using unpublished Monte-Carlo $g^{HS}(x, y)$ from Verlet and Schiff. In this way an accurate and extensive set of approximations in the form of extended virial series for n ranging from 4 to 24 was obtained. The details are given in Appendix A of this paper. These approximants are equally accurate and more convenient to use in subsequent work than the Padé approximants given earlier for some of these integrals [3]. We have also calculated the corresponding integrals obtained when $g^{HS}(x, y)$ is replaced by $g^{HS}(x, y) - 1$ for n ranging from -1 to 2. These are required in the next section where the Stell–Lebowitz theory [10] for charged particles is considered. Our extended virial series approximations for $I_n^{HS}(x)$ were also used in calculating the term of $O(\lambda^2)$ in the free energy of the dipolar–quadrupolar system [3]:

$$\beta f_2 = -x \left[\frac{\mu^{*4}}{6} I_6^{HS}(x) + \frac{\mu^{*2} \Theta^{*2}}{2} I_8^{HS}(x) + \frac{7\Theta^{*4}}{10} I_{10}^{HS}(x) \right]. \qquad (3.10)$$

The angular averaging of the three-body terms of $O(\lambda^3)$ represented by graphs in (2.14), has already been discussed by Rasaiah and Stell [20]. From this it follows that the corresponding contribution to the free energy is

$$\beta f_{3,3} = x^2 \left[\frac{\mu^{*6}}{54} I_{TD}^{HS}(x) + \frac{\mu^{*4} \Theta^{*2}}{480} I_{DDQ}^{HS}(x) + \frac{\mu^{*2} \Theta^{*4}}{640} I_{DQQ}^{HS}(x) \right.$$
$$\left. + \frac{\Theta^{*6}}{6400} I_{TQ}^{HS}(x) \right] \qquad (3.11)$$

where the triple integral is defined as

$$I_{triple}^{HS}(x) \equiv \int g_{123}^{HS}(R, s, r) W_{triple}(R, s, r) \, ds \, dr, \qquad (3.12)$$

in which $R = r_{12}/a$, $s = r_{13}/a$ and $r = r_{23}/a$. The individual angularly averaged three-body potentials, represented collectively as W_{triple} in (3.12), are precisely the same as the corresponding angular terms (W_{TD}, W_{DDQ}, W_{DQQ} and W_{TQ}) which occur in the theory of dispersion forces [15].

The triple integral (3.12) has been calculated here by employing the superposition approximation for $g_{123}^{HS}(R, s, r)$ and the procedure described in I for triple quadrupoles. Since the calculation is rather involved, the details are discussed in Appendices B and D. In this section we present only the results for the density expansion of $I_{triple}^{HS}(x)$ to $O(x^3)$ and an extension of this, which includes two additional powers of x. This extended virial approximation is sufficient to obtain agreement to within 0·5 per cent with a numerical calculation of the integral using the full $g^{HS}(r)$ in the superposition approximation. The series are convenient to use in subsequent calculations of the free energy at an

arbitrary fluid density. The coefficients of the extended virial series approximation

$$I_{\text{triple}}^{\text{HS}}(x) \simeq J_0 + J_1 x + J_2 x^2 + J_3 x^3 + J_4 x^4 + J_5 x^5, \qquad (3.13)$$

for the various three-body interactions are summarized in table 1. All of the J_0 coefficients in this table were obtained analytically, and so were the J_1 for triple–dipoles and triple–quadrupoles, and the J_2 and J_3 for the same systems when the Percus–Yevick (PY) radial distribution function was used for the reference system. The analytic results and numerical calculations of the coefficients in table 1 are discussed in Appendix B, and the numerical calculation of $I_{\text{triple}}^{\text{HS}}(x)$ is discussed in Appendix D.

The use of the PY approximation for the two-body radial distribution functions in the superposition approximation for $g_{123}^{\text{HS}}(R, s, r)$ generally tends to compensate for errors introduced by the latter approximation [21], and we have accordingly used the appropriate extended virial series based on the J_0, J_1, J_2^{PY} and J_3^{PY} coefficients in all our calculations of the three-body terms of $O(\lambda^3)$. The difference between using this and the alternative set given in table 1 is very small—about 0·6 per cent in $I_{\text{TD}}^{\text{HS}}(x)$ at a reduced density $x = 0·8$. This corresponds to a 0·2 per cent difference in $\beta\Delta f^{\text{P}}$ at the same density, for $\mu^* = 1·0$ and $\Theta^* = 0$. With these approximations for $I_n^{\text{HS}}(x)$ and $I_{\text{triple}}^{\text{HS}}(x)$, the quantities

$$\beta f_3 = \beta(f_{3,2} + f_{3,3}) \qquad (3.14)$$

and f_2 can be easily calculated at any fluid density. Our results for a range of fluid densities are shown in figure 1 with the details supplied in table 2. Three systems are compared; (i) $\mu^* = \sqrt{2}$, $\Theta^* = 0$, (ii) $\mu^* = 0$, $\Theta^* = \sqrt{2}$ and (iii) $\mu^* = \Theta^* = 1$. The Padé approximant for the excess free energy (referring to hard spheres as the reference system),

$$\beta\Delta f^{\text{P}} \equiv \beta(f^{\text{P}} - f^0) = \beta f_2 \left[1 - \frac{f_3}{f_2} \right]^{-1}, \qquad (3.15)$$

which is our best estimate for the excess free energy of hard spheres with point-dipole and point-quadrupoles, is also shown in the same figure.

It is also of interest to calculate the excess energy per particle, which is $\beta\Delta e$ (in reduced units), and the excess compressibility factor Δz, since they are often more readily accessible experimentally than the excess free energy ($\beta\Delta f$). We have made use of the excess compressibility factor to locate the densities and pressure of co-existing fluid phases from a plot of the chemical potential against the pressure. These properties can be calculated from $\beta\Delta f$, Δz and the equation of state for hard spheres, for which we have used the Carnahan–Starling equation [22]. By applying the standard thermodynamic relations,

$$\Delta e = \frac{\partial(\beta\Delta f)}{\partial \beta} \qquad (3.16)$$

and

$$\Delta z = \frac{x\partial(\beta\Delta f)}{\partial x} \qquad (3.17)$$

to the free energy series, we have

$$\Delta e = e_2 + e_3 + \dots \qquad (3.18)$$

Table 1. Coefficients of the extended virial series approximation for $I_{triple}^{HS}(x)$ (equation (3.13)). All J_n; $n \geq 1$ are determined within the context of the superposition approximation. Superscripts 'PY' and 'ex' refer to the use of the density expansion of the Percus–Yevick or the exact radial distribution function for hard spheres. The coefficients J_4 and J_5 are determined by a least squares fit of (3.13) to the results from a direct, numerical calculation of $I_{triple}^{HS}(x)$.

System	J_0	J_1	J_2^{PY}	J_3^{PY}	J_4^{PY}	J_5^{PY}	J_2^{ex}	J_3^{ex}	J_4^{ex}	J_5^{ex}
TD	16·4493	19·8096	6·3321	−0·0932	−1·1741	−0·8321	7·4085	−1·0792	−0·9901	−1·0249
DDQ	139·4906	241·9354	163·9581	57·0537	13·2686	−22·3827	178·2237	55·8448	12·4629	−34·4187
DQQ	139·4906	298·9225	283·4908	161·7222	81·7788	−35·8868	302·3091	171·8428	90·2115	−70·2773
TQ	532·9586	1287·3491	1447·9762	1026·3847	608·4235	−20·5065	1533·9543	1110·5044	720·1578	−248·8879

Table 2. Contributions to the excess free energy for hard spheres with point-dipoles and point-quadrupoles.

x	$\mu^* = \sqrt{2}$, $\Theta^* = 0$				$\mu^* = 0$, $\Theta^* = \sqrt{2}$					$\mu^* = 1$, $\Theta^* = 1$				
	βf_2	$\beta f_{3,3}$	$\beta(f_2+f_3)$	$\beta\Delta f^P$	βf_2	$\beta f_{3,2}$	$\beta f_{3,3}$	$\beta(f_2+f_3)$	$\beta\Delta f^P$	βf_2	$\beta f_{3,2}$	$\beta f_{3,3}$	$\beta(f_2+f_3)$	$\beta\Delta f^P$
0·1	−0·2990	0·0274	−0·2716	−0·2739	−0·5548	0·1378	0·0085	−0·4085	−0·4390	−0·3505	0·1349	0·0106	−0·2050	−0·2476
0·3	−1·0228	0·3060	−0·7168	−0·7873	−2·0386	0·5246	0·1218	−1·3922	−1·5478	−1·2556	0·5048	0·1328	−0·6180	−0·8327
0·5	−1·9394	1·0306	−0·9088	−1·2664	−4·1864	1·1264	0·5326	−2·5274	−2·9982	−2·5068	1·0610	0·5062	−0·9396	−1·5424
0·7	−3·0775	2·3932	−0·6843	−1·7312	−7·2554	2·0647	1·6158	−3·5749	−4·8136	−4·2126	1·8920	1·3441	−0·9765	−2·3824
0·8	−3·7379	3·3705	−0·3674	−1·9655	−9·2371	2·7149	2·6061	−3·9161	−5·8609	−5·2770	2·4486	2·0320	−0·7964	−2·8538
0·9	−4·4633	4·5690	0·1057	−2·2055	−11·5826	3·5273	4·0500	−4·0053	−7·0019	−6·5075	3·1285	2·9648	−0·4142	−3·3613
1·0	−5·2556	5·9984	0·7428	−2·4544	−14·3492	4·5416	6·1032	−3·7044	−8·2380	−7·9247	3·9491	4·2012	0·2256	−3·9068

B. Larsen *et al.*

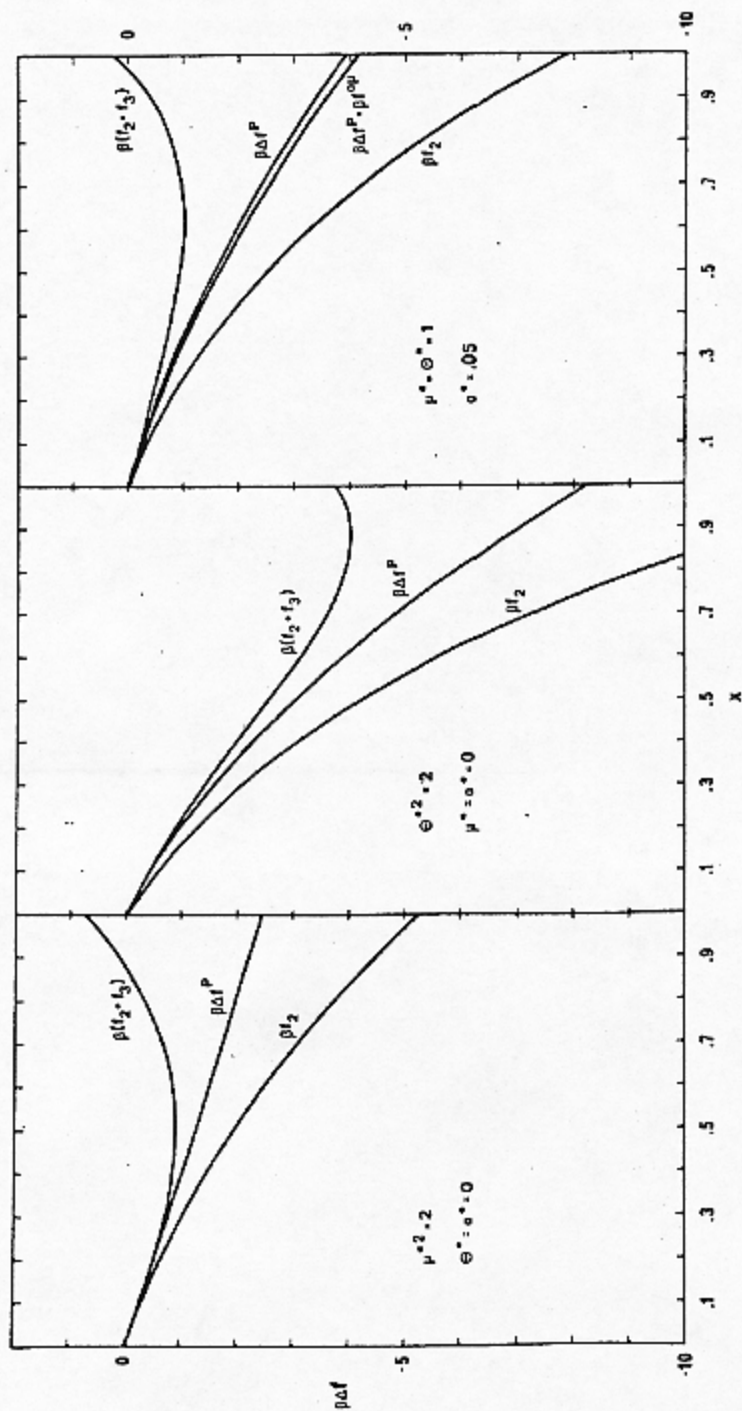
Figure 1. Excess free energies for polarizable hard spheres with point-dipoles and point-quadrupoles.

and

$$\Delta z = z_2 + z_3 + \dots, \tag{3.19}$$

where the subscripts 2 and 3 denote the terms of $O(\lambda^2)$ and $O(\lambda^3)$, respectively. From these one can form the Padé approximants

$$(\beta \Delta e)_{P1} = \frac{\beta e_2}{\left(1 - \dfrac{e_3}{e_2}\right)} \tag{3.20}$$

and

$$(\Delta z)_{P1} = \frac{z_2}{\left(1 - \dfrac{z_3}{z_2}\right)}. \tag{3.21}$$

The terms of $O(\lambda^2)$ and $O(\lambda^3)$ in the series for $\beta \Delta e$ are particularly simple since we are dealing with a hard sphere reference system whose properties are independent of the temperature. Taking account of the fact that β enters the expression for $\beta \Delta f$ only through μ^{*2} and Θ^{*2}, it follows immediately from (3.16) and the definitions of μ^{*2} and Θ^{*2} that

$$\beta \Delta e = \mu^{*2} \frac{\partial(\beta \Delta f)}{\partial(\mu^{*2})} + \Theta^{*2} \frac{\partial(\beta \Delta f)}{\partial(\Theta^{*2})}. \tag{3.22}$$

From this we find a simple prescription for the calculation of βe_n:

$$e_n = n f_n \quad (n \leqslant 3). \tag{3.23}$$

The factor n in (3.23) shows that the rate of convergence of the series for $\beta \Delta e$ is slower than for the series representing $\beta \Delta f$. When using Padé approximants for the series summation, however, the rate of convergence may be of little importance (provided the series converges at all). *A priori* there is no reason to prefer one series over the other in this respect, but it is known from computer simulation results [4], that the thermodynamic properties are most accurately obtained via the free energy Padé. It seems advisable therefore, to calculate $\beta \Delta e$ by differentiating the free energy Padé. A second approximation for $\beta \Delta e$ given by

$$(\beta \Delta e)_{P2} = \beta (2f_2 - f_3) / \left(1 - \frac{f_3}{f_2}\right)^2 \tag{3.24}$$

is then obtained. Similar considerations also apply to the excess compressibility factor, for which a second, hopefully better, approximation is

$$(\Delta z)_{P2} = \frac{z_2}{\left(1 - \dfrac{f_3}{f_2}\right)} + \frac{1}{\left(1 - \dfrac{f_3}{f_2}\right)^2} \left[z_3 - \frac{f_3}{f_2} z_2\right]. \tag{3.25}$$

The prescriptions for z_2 and z_3 are also simple; they are given by the corresponding equations for βf_2 and βf_3 with $I_n{}^{HS}(x)$ replaced by

$$\left[I_n{}^{HS}(x) + x \frac{\partial}{\partial x} I_n{}^{HS}(x)\right]$$

and $I_{\text{triple}}^{\text{HS}}(x)$ replaced by

$$\left[2I_{\text{triple}}^{\text{HS}}(x) + x\,\frac{\partial}{\partial x}\,I_{\text{triple}}^{\text{HS}}(x)\right].$$

Our extended virial series approximations for these integrals allow us to calculate z_2 and z_3 with very little effort. A comparison between the two approximations for $\beta\Delta e$ and Δz at $\mu^* = \Theta^* = 1\cdot0$ is given in table 3.

Table 3. Comparison between two approximations for excess energy, $\beta\Delta e$, and excess compressibility factor, Δz, for hard spheres with point-dipoles and point-quadrupoles with $\mu^* = \Theta^* = 1\cdot0$. The P1 approximation is based on the series expansion of the actual property listed, the P2 approximation is based on differentiation of the free energy Padé.

x	$(\beta\Delta e)_{\text{P1}}$	$(\beta\Delta e)_{\text{P2}}$	$(\Delta z)_{\text{P1}}$	$(\Delta z)_{\text{P2}}$
0·1	−0·4319	−0·4226	−0·2625	−0·2623
0·3	−1·4255	−1·3850	−0·9763	−0·9697
0·5	−2·5872	−2·4915	−1·9718	−1·9344
0·7	−3·9145	−3·7298	−3·2929	−3·1768
0·8	−4·6418	−4·3971	−4·0926	−3·9131
0·9	−5·4138	−5·0975	−4·9961	−4·7353
1·0	−6·2334	−5·8328	−6·0127	−5·6529

We will now turn to the effects of polarization. Using Barker's formalism [9], McDonald [4] found that the additional free energy brought about by dipole-induced dipole interactions is

$$f^{x\mu} = f_{2,11} + f_{3,12} + f_{3,21} + \dots \tag{3.26}$$

In (3.26), the first subscript characterizes each term as a two-body or three-body contribution, while the next two subscripts give the orders of α (the polarizability) and μ^2, respectively. After doing the necessary angular integrals, McDonald showed that $f_{2,11}$ is related to the two-body dipole–dipole term of $O(\lambda^2)$ and $f_{3,12}$ and $f_{3,21}$ are related to the three-body triple–dipole term of $O(\lambda^3)$. Explicitly, for a hard sphere reference system,

$$\beta f_{2,11} = -\alpha^*\,\mu^{*2}\,x I_6^{\text{HS}}(x), \tag{3.27}$$

$$\beta f_{3,12} = \frac{\alpha^*\,\mu^{*4}\,x^2}{6}\,I_{\text{TD}}^{\text{HS}}(x) \tag{3.28}$$

and

$$\beta f_{3,21} = \frac{\alpha^{*2}\,\mu^{*2}\,x^2}{2}\,I_{\text{TD}}^{\text{HS}}(x), \tag{3.29}$$

where $\alpha^* = \alpha/a^3$. The last term is quite small for typical polar fluids (e.g. HCl; $\alpha^* \simeq 0\cdot05$) and can be ignored. Hence $\beta f^{x\mu}$ may be considered to be a power series in $\alpha^*\,\mu^{*2n}$, and McDonald sums this in the same spirit as our Padé

approximant for permanent dipoles and multipoles to get

$$f^{x\mu} = f_{2,11} \left[1 - \frac{f_{3,12}}{f_{2,11}} \right]^{-1}. \tag{3.30}$$

The corresponding contribution to the excess compressibility factor, $z^{x\mu}$, is given by an expression exactly analogous to (3.25) with $z_{2,11}$ and $z_{3,12}$ replacing z_2 and z_3, where $z_{2,11}$ and $z_{3,12}$ are related to $f_{2,11}$ and $f_{3,12}$ in the same way as z_2 and z_3 are related to f_2 and f_3. Our best approximation for the dipole-induced dipole contribution to the reduced energy is

$$(\beta e^{x\mu})_{P2} = \beta f_{2,11} \left[1 - \frac{f_{3,12}}{f_{2,11}} \right]^{-2}. \tag{3.31}$$

This is the analogue of (3.24), but has a different functional form since, instead of (3.23), we have

$$e_{2,11} = f_{2,11} \quad \text{and} \quad e_{3,12} = 2 f_{3,12}. \tag{3.32}$$

We have calculated the free-energy contribution according to (3.30) when $\mu^* = \Theta^* = 1{\cdot}0$ and $\alpha^* = 0{\cdot}05$. The results are given in figure 1 and table 4. It is found that the polarization effect accounts for less than 10 per cent of the total excess free energy in this case.

Table 4. Contributions to the excess free energy due to polarizability for hard spheres with permanent dipole moment $\mu^* = 1{\cdot}0$ and polarizability $\alpha^* = 0{\cdot}05$.

x	$\beta f_{2,11}$	$\beta f_{3,12}$	$\beta f_{3,21}$	$\beta(f_{2,11} + f_{2,12})$	$\beta f^{x\mu}$
0·1	−0·0224	0·0015	0·0002	−0·0209	−0·0210
0·3	−0·0767	0·0172	0·0026	−0·0595	−0·0627
0·5	−0·1455	0·0580	0·0087	−0·0875	−0·1040
0·7	−0·2308	0·1346	0·0202	−0·0962	−0·1458
0·8	−0·2803	0·1896	0·0284	−0·0907	−0·1672
0·9	−0·3348	0·2570	0·0386	−0·0778	−0·1894
1·0	−0·3942	0·3374	0·0506	−0·0568	−0·2124

The liquid–vapour co-existence curves in the critical region are shown in figure 2 for four special cases of the present model; (i) $\Theta^* = \alpha^* = 0 < \mu^*$, (ii) $\mu^* = \alpha^* = 0 < \Theta^*$, (iii) $\mu^* = \Theta^* > 0 = \alpha^*$, and (iv) $\mu^* = \Theta^* > 0$, $\alpha^* = 0{\cdot}05$. A large difference between the purely dipolar and the purely quadrupolar system is observed. The critical point of the quadrupolar system is located at values of T^* and x that are 100 per cent higher than those for the dipolar system. Dipole moments added to the quadrupoles so that $\mu^* = \Theta^*$ increase the critical temperature and decrease the critical density by 20 per cent. The polarization has little effect on the position of the critical point. The rectilinear diameters are considerably more temperature dependent for the dipolar system than the others. For the purely quadrupolar system, the rectilinear diameter shows a slight curvature, whereas it is practically linear in the other cases. Our estimates of the critical constants are given in table 5. We should also point out that in the cases where quadrupoles are involved, the value of z_c differs considerably from the 'normal' value 0·3.
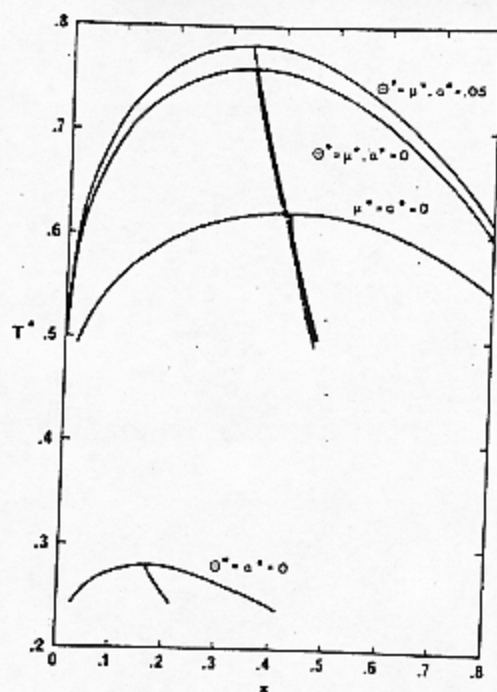
B. Larsen *et al.*

Figure 2. Liquid–vapour co-existence curves for polarizable hard spheres with point-dipoles and point-quadrupoles. The reduced temperature T^* is defined as $1/\mu^{*2}$ when $\Theta^* = 0$ or $\Theta^* = \mu^*$, and as $1/\Theta^{*2}$ when $\mu^* = 0$.

Table 5. .. Estimates of the critical constants for polarizable hard spheres with permanent dipoles and/or quadrupoles.

Case	μ^*	Θ^*	α^*	T_c^* (a)	x_c	z_c (b)
(i)	> 0	0	0	0·28	0·165	0·300
(ii)	0	> 0	0	0·62	0·420	0·473
(iii)	> 0	μ^*	0	0·76	0·340	0·421
(iv)	> 0	μ^*	0·05	0·78	0·335	0·409

(i) $\Theta^* = \alpha^* = 0 < \mu^*$; (ii) $\mu^* = \alpha^* = 0 < \Theta^*$; (iii) $\mu^* = \Theta^* > 0 = \alpha^*$; (iv) $\mu^* = \Theta^* > 0$, $\alpha^* = 0.05$.

(a) $T^* \equiv 1/\mu^{*2}$ in cases (i), (iii) and (iv), and $\equiv 1/\Theta^{*2}$ in case (ii).

(b) $z_c \equiv p_c V_c / N k_B T_c$.

4. MIXED PERTURBATION THEORY FOR CHARGED SYSTEMS

In this section the thermodynamic properties of charged systems are discussed by employing a mixed perturbation theory with the Stell–Lebowitz (SL) [10] and Mayer [13] expansions as the ingredients in the mixture. Both these theories are, of course, exact if evaluated to all orders in their respective ordering parameters, which are the ionic number density ρ in the Mayer expansion and the charge parameter $\beta e^2/\epsilon$ in the SL theory. Here we shall consider the union

of the Mayer expansion truncated after its second term and a Padé approximant based upon the SL expansion of the Helmholtz free energy through $O(\kappa^6)$.

Our discussion is limited to the simplest possible case, namely an electrically neutral system of ions which are identical in all respects except for the charges. The numerical results presented are for the restricted primitive model (RPM), i.e. charged hard spheres of diameter a, immersed in a continuum of dielectric constant ϵ. For this system, the leading terms in a free-energy expansion derived by Stell and Lebowitz [10] are

$$(\beta f)_{\mathrm{SL6}} = \beta f^0 - \frac{\kappa^3}{12\pi\rho} - \frac{\kappa^4}{16\pi\rho} \int_0^\infty h_{12}^0 \, dr + \frac{\kappa^5}{8\pi\rho} \int_0^\infty h_{12}^0 \, r \, dr - \frac{\kappa^6}{8\pi\rho}\left[\int_0^\infty h_{12}^0 \, r^2 \, dr \right.$$

$$\left. - \tfrac{1}{6} \int_0^\infty dr_{12} \int_0^\infty dr_{13} \int_{|r_{13}-r_{12}|}^{r_{12}+r_{13}} h_{123}^0 \, dr_{23} \right]. \quad (4.1)$$

The subscript 6 is associated with SL to emphasize our interest only in a finite number of terms (to $O(\kappa^6)$) in the SL expansion, so that SL6 constitutes an approximation to the exact result. In (4.1), βf is the reduced Helmholtz free energy per particle, βf^0 is the corresponding free energy of the reference system, $-\kappa^3/12\pi\rho$ is the Debye–Hückel limiting law (DHLL) term with κ equal to the reciprocal Debye length, defined by

$$\kappa^2 = (4\pi e^2 \beta/\epsilon) \sum_{\substack{\text{all ionic} \\ \text{species}}} z_i^2 \, \rho_i,$$

where ρ_i is the density of species i, and $\rho = \sum \rho_i$. The remaining terms contain h_{12}^0 and h_{123}^0 which are two and three-particle correlation functions for the reference system, and ρ is the total number density of the ions. Details dealing with the calculations of the integrals in (4.1) when applied to the RPM are given in Appendices A, C and D. Like our treatment of polar molecules in § 3, the density expansions of h_{12}^0 and h_{123}^0 are used together with the superposition approximation for the latter to arrive at the following extended virial approximations for these integrals :

$$\int_0^\infty h_{12}^{\mathrm{HS}} \, dr = a(-1 + 0.4581x - 0.2686x^2 + 0.1543x^3$$

$$- 0.0733x^4 + 0.0168x^5), \quad (4.2)$$

$$\int_0^\infty h_{12}^{\mathrm{HS}} \, r \, dr = a^2(-0.5 + 0.5760x - 0.5911x^2 + 0.5428x^3$$

$$- 0.4163x^4 + 0.1630x^5), \quad (4.3)$$

$$\int_0^\infty h_{12}^{\mathrm{HS}} \, r^2 \, dr = a^3(-0.3333 + 0.7418x - 1.2047x^2 + 1.6139x^3$$

$$- 1.5487x^4 + 0.6626x^5) \quad (4.4)$$

and

$$\int_0^\infty dr_{12} \int_0^\infty dr_{13} \int_{|r_{13}-r_{12}|}^{r_{12}+r_{13}} h_{123}^{\mathrm{HS}} \, dr_{23} = a^3(1.5 - 2.3431x + 2.8107x^2$$

$$- 3.1292x^3 + 2.6899x^4 - 1.0081x^5). \quad (4.5)$$

The first four coefficients in (4.5) have been evaluated analytically using the Percus–Yevick theory for h_{12}^{HS} ; in the exclusively two-body integrals the

B. Larsen *et al.*

density expansion for the exact $h_{12}{}^{HS}$ has been used. The last two terms in each series have been determined from a least squares fit to the directly calculated values of the integrals.

Our calculations of the triple integral go beyond the work of Stell and Wu [12] who computed the coefficients up to $O(x^2)$ only, but unlike them, we do not take corrections to the superposition approximation into consideration. According to Stell and Wu, the best Padé approximant based on (4.1) is of the form

$$(\beta \Delta f)_{SL6(P)} = -\frac{\kappa^3}{12\pi\rho} \frac{1 + n_1\kappa}{1 + d_1\kappa + d_2\kappa^2},$$

(4.6)

where the coefficients n_1, d_1 and d_2 are independent of the temperature, and determined so as to reproduce (4.1) correctly on expansion. For the value of $\beta e^2/\epsilon$ corresponding to a 2-2 aqueous electrolyte model at room temperature, the convergence of the SL expansion is extremely slow at concentrations above 0.25 molar. This is illustrated in figure 3 where different approximations to $\beta \Delta f$ are shown as functions of the ionic strength

$$I = \frac{1}{2} \sum_{\substack{\text{all ionic} \\ \text{species}}} \rho_i z_i^2.$$

The reason why the SL6(P) approximation works at all seems to be that it is heavily biased by its asymptotic form of linear $\beta e^2/\epsilon$ dependence as $\beta e^2/\epsilon \to \infty$,
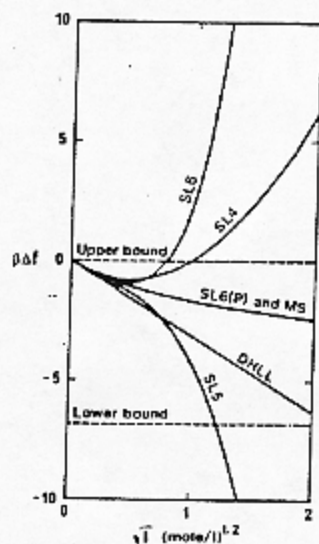

Figure 3. Different approximations for the excess free energy for the restricted primitive model (charged hard spheres) versus the square root of the ionic strength for 2-2 electrolytes with $a = 4.2$ Å, $t = 25°$ C and $\epsilon = 78.358$. DHLL refers to the Debye–Hückel limiting law, curves 'SL4' and 'SL5' are the free energies to $O(\kappa^4)$ and $O(\kappa^5)$ in the Stell–Lebowitz expansion, and 'SL6' is the free energy to $O(\kappa^6)$ given by equation (4.1). The Padé approximant (4.6) based on (4.1), and the mean spherical approximation give the indistinguishable results on this scale, 'SL6(P) and MS'. The two bounds shown are Rasaiah and Stell's upper bound, $\beta \Delta f \leq 0$, and Onsager's lower bound, $\beta \Delta f \geq -\beta e^2/\epsilon a$.

which is known to be correct. The close agreement between the SL6(P) and the mean spherical [23] (MS) approximations is owing to additional similarities between the two theories. In figure 3 two existing bounds on $\beta \Delta f$ are shown: Rasaiah and Stell's upper bound [24], $\beta \Delta f \leqslant 0$, and Onsager's lower bound [25] $\beta \Delta f \geqslant -\beta e^2/\epsilon a$. In the limit of $\beta e^2/\epsilon \rightarrow \infty$, the MS result approaches Onsager's lower bound asymptotically at all $\rho > 0$, whereas the SL6(P) result tends to a value somewhere between the two bounds, the exact limit being determined by the density.

By differentiating (4.6) with respect to the density and temperature, we get the additional results for the compressibility factor z (which is identical to the osmotic coefficient for this model electrolyte) and excess energy $\beta \Delta e$ of 1–1 and 2–2 model electrolytes that are presented in tables 6 and 7. The comparison with Monte Carlo [26] and other results [23, 27] shows that the SL6(P) is already quite good for 1–1 electrolytes at all concentrations up to 2 molar (corresponding to a reduced density $x \simeq 0.2$). For 2–2 electrolytes the theory is less satisfactory at these concentrations.

A more serious flaw is that none of the anomalous effects shown by real 2–2 electrolytes in the very low concentration region (lower than the region covered by table 7), such as negative deviations from the DHLL for the osmotic coefficient, appear in SL6(P). The leading terms in the Mayer expansion are the DHLL term ($\kappa^3/12\pi\rho$) and the renormalized second virial coefficient $B_2(\kappa)$. The sum of these two, known as the DHLL + B_2 approximation, behaves quite differently from the SL6(P) when applied to 2–2 electrolytes at low concentrations. This difference is illustrated in figure 4. The reduced free energy in the DHLL + B_2 approximation is, relative to the ideal gas,

$$(\beta f)_{\text{DHLL}+B_2} = -\frac{\kappa^3}{12\pi\rho} + \frac{B_2(\kappa)}{\rho}, \qquad (4.7)$$

where

$$B_2(\kappa) = -2\pi \sum_{i=1}^{\sigma} \sum_{j=1}^{\sigma} \rho_i \rho_j \int_0^\infty \left[(1+f_{ij}^0)\exp{(q_{ij})} - 1 - \frac{q_{ij}^2}{2} \right] r^2\, dr, \qquad (4.8)$$

and

$$q_{ij} = -\beta e_i e_j \exp{(-\kappa r)}/\epsilon r, \qquad (4.9)$$

$$f_{ij}^0 = \exp{(-\beta u_{ij}^0)} - 1,$$

is the Mayer f-function of the reference system. In (4.9) $e_i = z_i e$, is the charge on the ith ionic species whose number density is ρ_i, ϵ is the dielectric constant of the solvent and σ is the total number of ionic species.

It is clear from inspection that the $\kappa^3/12\pi\rho$ and the term

$$-2\pi \sum\sum \rho_i \rho_j \int_0^\infty f_{ij}^0 \left[1 + \frac{q_{ij}^2}{2} \right] r^2\, dr \qquad (4.10)$$

are included in SL6 and hence SL6(P), and it is equally clear that the rest of B_2 is not included in SL6. It is not as immediately clear whether the terms in SL6(P) beyond SL6 itself include any further contributions from B_2, but a comparison of the relative orders in x and $\beta e^2/\epsilon a$ of SL6(P) with the rest of B_2 shows that they are indeed disjoint, so that one can identify the expression given in (4.10) as SL(P)$\cap B_2$.

Table 6. Thermodynamic properties of a 1–1 restricted primitive model electrolyte ($a = 4\cdot25$ Å, $\epsilon = 78\cdot5$, $d\epsilon/dT = 0$, $T = 298\cdot16$ K).

C_{st} (a) (moles/litre)	$z = pV/Nk_BT$				$-\beta\Delta e$			
	MS	SL6(P)	SL6(P)∪B₂	MC	MS	SL6(P)	SL6(P)∪B₂	MC
0·00911	0·9709	0·9706	0·9703	0·9701 ± 0·0008	0·0992	0·0992	0·1012	0·1029 ± 0·0013
0·10376	0·9454	0·9453	0·9455	0·9445 ± 0·0012	0·2675	0·2674	0·2702	0·2739 ± 0·0014
0·42502	0·9806	0·9800	0·9805	0·9774 ± 0·0046	0·4264	0·4260	0·4267	0·4341 ± 0·0017
1·0001	1·097	1·094	1·094	1·094 ± 0·005	0·5405	0·5398	0·5399	0·5516 ± 0·0016
1·9676	1·360	1·349	1·349	1·346 ± 0·009	0·6362	0·6375	0·6375	0·6511 ± 0·0020

(a) Stoichiometric concentration $C_{st} = \rho/2\cdot\mathscr{N}$ where $\mathscr{N}$ is Avogadro's number, $\mathscr{N} = 6\cdot0225 \times 10^{23}$.

Table 7. Thermodynamic properties of a 2–2 restricted primitive model electrolyte ($a = 4\cdot2$ Å, $\epsilon = 78\cdot358$, $d\epsilon/dT = 0$, $T = 298\cdot16$ K).

C_{st} (a) (moles/litre)	$z = pV/Nk_BT$				$-\beta\Delta e$				
	MS	SL6(P)	SL6(P)∪B₂	ORPA+B₂ (b)	MS	SL6(P)	SL6(P)∪B₂	ORPA+B₂ (b)	MC
0·0625	0·6303	0·6322	0·6811	0·643	1·455	1·452	1·599	2·062	1·900 ± 0·017
0·25	0·5543	0·5652	0·5814	0·588	2·178	2·153	2·159	2·564	2·447 ± 0·014
0·5625	0·5732	0·5931	0·5957	0·595	2·643	2·586	2·586	2·916	2·821 ± 0·008
1·0	0·6520	0·6735	0·6738	0·652	2·979	2·890	2·890	3·199	3·082 ± 0·01
2·0	0·9112	0·9075	0·9075	0·857	3·380	3·225	3·255	3·579	3·522 ± 0·012

(a) See footnote to table 6.
(b) ORPA+B₂ from S. Hudson and H. C. Andersen, 1974, J. Chem. Phys., 60, 2188.
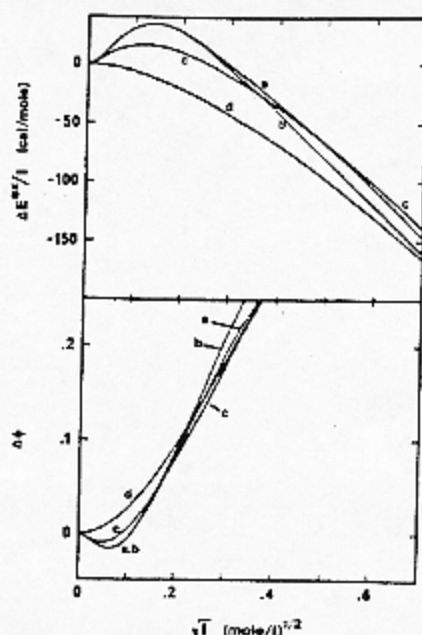
Figure 4. Approximations for the excess energy and osmotic coefficient for charged hard
spheres versus the square root of the ionic strength for 2–2 electrolytes with $a =$
4·2 Å, $t = 25°$ C, $\epsilon = 78·358$ and $\partial \ln \epsilon/\partial \ln T = -1·3679$. The energy symbol E
means energy per unit volume, and Δ is in this figure used to denote the difference
between actual approximation and the Debye–Hückel limiting law. Curve a is
the DHLL + B_2 approximation (4.7), curve b the SL6(P)∪B_2 and MS∪B_2 approxi-
mations of reference [14], curve c the hypernetted chain results of Rasaiah [28], and
curve d the SL6(P) and MS results. Notice that the anomalous deviation from the
DHLL in the energy is *positive* when $\partial \ln \epsilon/\partial \ln T < -1·0$. I is the ionic strength.

Defining

$$\Delta B_2 = B_2 - \text{SL6(P)} \cap B_2 \tag{4.11}$$

we have

$$\text{SL6(P)} \cup B_2 = \text{SL6(P)} + B_2 - \text{SL6(P)} \cap B_2$$
$$= \text{SL6(P)} + \Delta B_2, \tag{4.12}$$

where

$$\Delta B_2 = -2\pi \sum_{i=1}^{\circ} \sum_{j=1}^{\circ} \rho_i \rho_j \int_0^\infty (1 + f_{ij}^{\,0}) \left(\exp(q_{ij}) - 1 - \frac{q_{ij}^{\,2}}{2} \right) r^2 \, dr. \tag{4.13}$$

A similar analysis shows that the corresponding ΔB_2 for the mean spherical
approximation is also given by (4.13).

Since $\Delta B_2 \to 0$ as $\beta e^2/\epsilon \to \infty$ when $\rho > 0$, the SL6(P)∪B_2 approximation
(4.12) saturates as the SL6(P) approximation in this limit. The SL6(P)∪B_2
also has the correct limiting behaviour of DHLL + B_2 as $\beta e^2/\epsilon \to 0$ or $\rho \to 0$.
Moreover, the SL6(P)∪B_2 gives essentially the same deviation from the DHLL
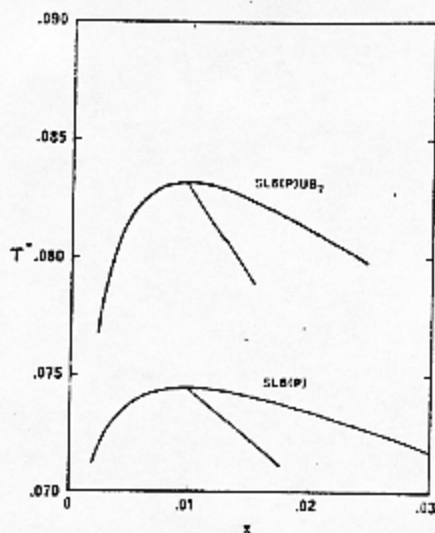as does the DHLL + B_2. This is clearly apparent in figure 4 which shows the

B. Larsen *et al.*

Figure 5.   Co-existence curves for the RPM as predicted by the SL6(P) and SL6(P)∪B_2 approximations.   The reduced temperature T^* is here defined as $\epsilon a/\beta e^2$ and $x = \rho a^3$ is the reduced density.

deviations from the DHLL of the excess energy and osmotic coefficient in different approximations [23, 28] for the 2–2 electrolyte model†.   The SL6(P)∪B_2 approximation is, in general, an improvement of the SL6(P) approximation for the cases of 1–1 and 2–2 electrolytes.   Results are summarized in tables 6 and 7.   At the higher concentrations, we note that the ΔB_2 correction vanishes for both systems.

Recently Stell *et al.* discovered compelling evidence for a phase transition in the restricted primitive model involving a critical point at very low density [14]‡.   The SL6(P)∪B_2 is an approximation that should be well suited to mapping out the qualitative features of the phase surface over a wide range of T and x, and we have used it here to explore the critical region, along with the SL6(P) for purposes of comparison.   Both approximations yield a critical point. The co-existence curves are shown in figure 5.   Our estimates of the critical constants are $T_c^* = 0.0745$, $x_c = 0.0098$, and $z_c = 0.091$ in the SL6(P) approximation, and $T_c^* = 0.0832$, $x_c = 0.0096$, and $z_c = 0.38$ in the SL6(P)∪B_2 approximation where $T^* \equiv \epsilon a/\beta e^2$ and $x = \rho a^3$.

† The excess energy E^{ex} is the internal energy per unit volume for the system multiplied by $(1 + \partial \ln \epsilon/\partial \ln T)$, where ϵ is the dielectric constant and T is the temperature. E^{ex}/I, where I is the ionic strength, is proportional to the heat of dilution [28].

‡ We take this opportunity to call attention to the fact that the transcription of Larsen's equation given by Stell and Wu [12] contains several misprints : In their equation (11.6) $b(\eta)$ should be $b(\eta)\Gamma^{1/2}$.   Immediately below that equation Γ should be $2(ze)^2 \eta^{1/4}/\epsilon akT$, and $4^{1/4}7/12$ is the coefficient of $\eta^{1/4}$, not η, in the expression for $b(\eta)/d(\eta)$.

College (University of London) and at Oxford University, where the work was completed.

APPENDIX A

The density expansion and extended virial approximation of two-body integrals $I_n^{HS}(x)$.

The first terms of the density expansion of the hard-sphere radial distribution function are [29, 30]

$$g^{HS}(x, y) = \exp\left[-\beta u^{HS}(y)\right][1 + xg_1(y) + x^2 g_2(y) + x^3 g_3(y) + O(x^4)], \quad (A\,1)$$

where $u^{HS}(y)$ is the hard-sphere pair potential.

One has a simple analytic expression for the coefficient $g_1(y)$, and convenient tabulations of $g_2(y)$ and $g_3(y)$ are provided by Ree *et al.* [31]. Substitution of (A 1) into the definition of the two-body integral $I_n^{HS}(x)$, (3.9), yields a density expansion of $I_n^{HS}(x)$:

$$I_n^{HS}(x) = \sum_{i=0}^{3} J_{i,n}\, x^i + O(x^4). \qquad (A\,2)$$

The coefficients $J_{0,n}$ and $J_{1,n}$ may be found analytically as

$$J_{0,n} = \frac{4\pi}{n-3}\; ; \quad n \geqslant 4 \qquad (A\,3)$$

and

$$J_{1,n} = \pi^2 \left(\frac{19}{6} - 4\ln 2\right) \qquad\qquad (n=4)$$

$$= \frac{\pi^2}{3}\left(\frac{1}{6} + \ln 2\right) \qquad\qquad (n=6)$$

$$= 4\pi^2 \left(\frac{2^{6-n}-1}{12(6-n)} - \frac{2^{4-n}-1}{4-n} + \frac{4(2^{3-n}-1)}{3(3-n)}\right) \quad (n=5 \text{ and } n > 6). \quad (A\,4)$$

The coefficients $J_{2,n}$ and $J_{3,n}$ have been calculated previously for $n = 6$, 8, 10, 12, 18 and 24 [3], and for $n = 15$ [1], but for the sake of completeness we present in table 8 the entire set with n ranging from 4 to 24. The numerical estimates of $J_{2,n}$ and $J_{3,n}$ have been obtained with the aid of a highly accurate version of the usual Simpson's integration rule. This version is discussed in Appendix D.

Since numerical tabulations of $g^{HS}(x, y)$ from Monte-Carlo calculations exist for several densities x, we have also calculated $I_n^{HS}(x)$ numerically from (3.9) for these densities, again using the Simpson's rule discussed in Appendix D. Combining the known density expansion of $I_n^{HS}(x)$, (A 2), with these results, an approximation for $I_n^{HS}(x)$ has been constructed in the form of an extended virial series:

$$I_n^{HS}(x) \simeq \sum_{i=0}^{5} J_{i,n}\, x^i. \qquad (A\,5)$$

1010   B. Larsen *et al.*

Table 8. Coefficients of the density expansion of the two-body integral $I_n^{HS}(x)$ with $4 \leqslant n \leqslant 24$.

n	$J_{0,n}$	$J_{1,n}$	$J_{2,n}$	$J_{3,n}$	$J_{4,n}$	$J_{5,n}$	Max. error (per cent)
4	12·5664	3·8894	−0·0817	−0·0845	0·7512	−0·6802	0·1
5	6·2832	3·2899	0·5226	−0·0835	0·1077	−0·0963	0·1
6	4·1888	2·8287	0·8331	0·0317	0·0858	−0·0846	0·1
7	3·1416	2·4674	0·9823	0·1565	0·0901	−0·0734	0·2
8	2·5133	2·1795	1·0423	0·2596	0·1097	−0·0573	0·2
9	2·0944	1·9465	1·0533	0·3360	0·1355	−0·0369	0·2
10	1·7952	1·7551	1·0376	0·3890	0·1561	−0·0082	0·2
11	1·5708	1·5957	1·0079	0·4237	0·1740	0·0215	0·3
12	1·3963	1·4614	0·9716	0·4448	0·1846	0·0543	0·3
13	1·2566	1·3470	0·9326	0·4562	0·1906	0·0865	0·3
14	1·1424	1·2486	0·8934	0·4608	0·1921	0·1180	0·3
15	1·0472	1·1631	0·8552	0·4506	0·1913	0·1465	0·3
16	0·9666	1·0882	0·8186	0·4569	0·1864	0·1745	0·3
17	0·8976	1·0221	0·7841	0·4510	0·1801	0·1999	0·3
18	0·8378	0·9635	0·7517	0·4437	0·1723	0·2332	0·3
19	0·7854	0·9110	0·7213	0·4354	0·1637	0·2440	0·3
20	0·7392	0·8639	0·6930	0·4266	0·1546	0·2630	0·3
21	0·6981	0·8214	0·6666	0·4175	0·1450	0·2802	0·3
22	0·6614	0·7828	0·6420	0·4083	0·1353	0·2957	0·3
23	0·6283	0·7476	0·6191	0·3992	0·1259	0·3093	0·3
24	0·5984	0·7154	0·5977	0·3902	0·1165	0·3216	0·3

The coefficients $J_{4,n}$ and $J_{5,n}$ have been estimated by a least squares fit of (A 5) to the values of $I_n^{HS}(x)$ calculated from (3.9), and our results are given in table 8. The maximum deviation observed in the approximation (A 5) from the exact result is given in the last column of table 8.

The Stell–Lebowitz theory [10] applied to charged hard spheres involves integrals that are very similar to $I_n^{HS}(x)$. In particular, we need in § 4

$$I_n^{HS}(x) \equiv 4\pi \int_0^\infty [g^{HS}(x, y) - 1] y^{2-n} \, dy; \quad 0 \leqslant n \leqslant 2, \tag{A 6}$$

which, without the risk of confusion, may be taken as a definition of $I_n^{HS}(x)$ for $-1 \leqslant n \leqslant 2$. We have estimated these integrals, following the procedure described above, and the results are summarized in table 9. No serious discrepancies between these results and the results of Stell and Wu [12] has been

Table 9. Coefficients of the density expansion of the two-body integral $I_n^{HS}(x)$ with $-1 \leqslant n \leqslant 2$.

n	$J_{0,n}$	$J_{1,n}$	$J_{2,n}$	$J_{3,n}$	$J_{4,n}$	$J_{5,n}$	Max. error (per cent)
−1	−3·1416	12·3135	−30·0065	55·9888	(a)	(a)	(a)
0	−4·1888	9·3213	−15·1386	20·2804	−19·4618	8·3260	11·1
1	−6·2832	7·2377	−7·4281	6·8207	−5·2313	2·0478	1·2
2	−12·5664	5·7573	−3·3758	1·9396	−0·9212	0·2106	0·2

(a) No reasonably good fit of the extended virial approximation has been found.

found, and our results have been used in §4 because of the convenience of the extended virial approximation.

Appendix B
The density expansion for the triple integrals $I_{triple}^{HS}(x)$ using the superposition approximation

The triple integral $I_{triple}^{HS}(x)$ defined in (3.12) is evaluated here for triple-dipole (TD), dipole–dipole–quadrupole (DDQ) and dipole–quadrupole–quadrupole (DQQ) interactions by employing the superposition approximation (SA) for the three-particle correlation function $g_{123}^0(R, s, r)$, and the procedure described earlier for triple–quadrupoles (TQ) [1]. We also present some additional analytic results for triple–quadrupoles, viz. J_3^{DY}, which were not available earlier. Briefly, what we have done is to calculate the density (x) expansion for $I_{triple}^{HS}(x)$ up to $O(x^2)$ with aid of (A 1). We have also calculated the integral numerically using the full pair-correlation functions in the SA. This enables us to suggest an extended virial series approximation for $I_{triple}^{HS}(x)$, similar to the approximation for two-body integrals discussed in Appendix A.

By using the SA and bi-polar coordinates, (3.12) can be written as

$$I_{triple}^{HS}(x) = 8\pi^2 \int_1^2 \{II'(R; [g(s), g(r)]) + III(R; [g(s), g(r)])\}g(R) R\, dR$$

$$+ 8\pi^2 \int_2^\infty \{I(R; [g(s), g(r)]) + II(R; [g(s), g(r)])$$

$$+ III(R; [g(s), g(r)])\}g(R)R\, dR, \quad (B 1)$$

where it is understood without further specification that the radial distribution function $g(\ )$ refers to the hard-sphere system. The kernels in (B 1), e.g. $I(R; [g(s), g(r)])$, arise from the integration of (3.12) over different regions of r and s as shown in figure 6; the number of such regions depends on whether R is less than or greater than 2. The definitions of the kernels, which are given in I, will not be reproduced here, but it may be useful for the reader to recall
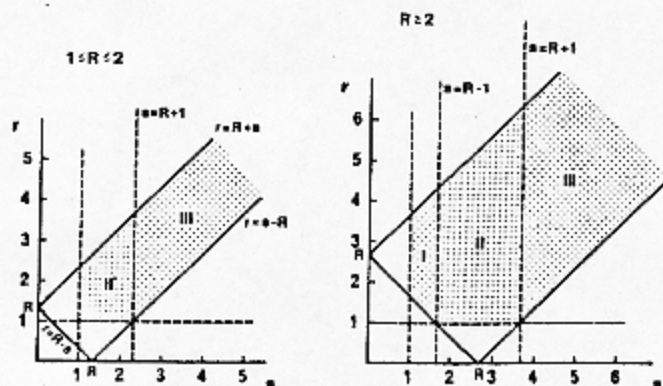

Figure 6. Integration regions of I_{triple}^{HS} with use of the superposition approximation for the three-particle correlation function g_{123}^{HS} and bi-polar coordinates (B 1).

that they are integrals over the variable s (see figure 6) of the product of $sg(s)$ and certain linear combinations of the functions $K(R+s\,;\ [g(r)])$, $K(R-s\,;\ [g(r)])$, $K(s-R\,;\ [g(r)])$ and $K(1\,;\ [g(r)])$, which are defined by the following indefinite integral over r :

$$K(q\,;\ [g(r)]) = \int^{q} g(r)W_{\text{triple}}(R,\,s,\,r)r\,dr. \qquad (\text{B 2})$$

The integrand in (B 2) contains the angularly averaged three-body potential $W_{\text{triple}}(R,\,s,\,r)$ [20].

By using the density expansion of the three hard-sphere distribution functions, (A 1), we get the first four terms in a density expansion for $I_{\text{triple}}^{\text{HS}}(x)$:

$$I_{\text{triple}}^{\text{HS}}(x) = J_0 + J_1 x + J_2 x^2 + J_3 x^3 + O(x^4). \qquad (\text{B 3})$$

If we denote g_0 by ———, g_1 by – – – –, g_2 by ········ and g_3 by ᜌᜌᜌᜌ, the coefficients J_n may be represented graphically as follows :

(a) for TD and TQ :

$$J_0 = \triangle \qquad (\text{B4}) \qquad J_1 = 3\,\triangle \qquad (\text{B 4, B 5})$$

$$J_2 = 3\,\triangle + 3\,\triangle \qquad (\text{B 6})$$

$$J_3 = 6\,\triangle + 3\,\triangle + \triangle \qquad (\text{B 7})$$

(b) for DDQ and DQQ :

$$J_0 = \triangle \qquad (\text{B8}) \qquad J_1 = 2\,\triangle + \triangle \qquad (\text{B 8, B 9})$$

$$J_2 = 2\,\triangle + \triangle + \triangle + 2\,\triangle \qquad (\text{B 10})$$

$$J_3 = 2\,\triangle + \triangle + 2\,\triangle + 2\,\triangle$$

$$+ 2\,\triangle + \triangle \qquad (\text{B 11})$$

All of these graphs represent integrals ; the vertices may be regarded as field points at which dipoles or quadrupoles reside, so that there is also an angularly averaged polar interaction and the factor $\exp\,(-\beta u^{\text{HS}})$ between adjacent vertices in addition to the g_0, g_1, g_2 or g_3 bond which links them. Under (a) an open circle denotes the presence of either a dipole or a quadrupole, and under (b) each large dark circle represents a dipole and each open circle represents a quadrupole in the case of DDQ triplet interactions, and vice versa for the DQQ triplet terms. In tables 10 and 11 our numerical and analytic estimates for each one of the integrals represented by a graph are given. These were obtained as follows :

From (A 1) and (B 1) we find that

$$J_0 = 8\pi^2 \int_{1}^{2} \{II'(R\,;\ [1,\,1]) + III(R\,;\ [1,\,1])\}R\,dR$$

$$+ 8\pi^2 \int_{2}^{\infty} \{I(R\,;\ [1,\,1]) + II(R\,;\ [1,\,1]) + III(R\,;\ [1,\,1])\}R\,dR \qquad (\text{B 12})$$

with analogous results for J_1, J_2 and J_3, as discussed below.

Table 10. Graphs which contribute to the density expansion of $I_{triple}^{HS}(x)$ for triple–dipoles (TD) and triple–quadrupoles (TQ).

			TD	TQ
J_0			16·4493	532·959
J_1			6·6032	429·116
J_2	PY		−1·7648	109·767
	exact		−1·4060	138·427
			3·8755	372·892
J_3	PY		−0·3017	121·846
	exact		−0·0794	147·614
	PY		−0·4001	−16·539
	exact		−1·1735	−40·035
			2·9173	344·927

o represents a dipole or quadrupole, and ——— $\equiv g_0$, $----\equiv g_1$, $\cdots\cdots\equiv g_2$ and $\sim\sim\sim\sim\equiv g_3$.

As in the case of triple–quadrupoles, it is found that

$$I(R; [g(s), 1]) = III(R; [g(s), 1]) = 0 \qquad (B\,13)$$

for all combinations of dipoles and/or quadrupoles. In particular, the analysis leading to (B 13) implies that

$$I(R; [g_n(s), 1]) = III(R; [g_n(s), 1]) = 0; \quad n = 0, 1, 2, 3. \qquad (B\,14)$$

From this it follows that for any combination of dipoles and/or quadrupoles,

$$J_0 = 8\pi^2 \int_1^2 II'(R; [1, 1])R\,dR + 8\pi^2 \int_2^\infty II(R; [1, 1])R\,dR. \qquad (B\,15)$$

Some further algebra leads to the following explicit results for the kernels:

$$II'(R; [1, 1]) = \begin{cases} -\tfrac{1}{24}(R - 6R^{-1}) & \text{for TD} \qquad (B\,16) \\ \tfrac{1}{2}(R^3 - 8R + 16R^{-1}) & \text{for DDQ and DQQ} \quad (B\,17) \\ \tfrac{1}{4}(5R^3 - 36R + 48R^{-1} + 64R^{-3}) & \text{for TQ} \qquad (B\,18) \end{cases}$$

and

$$II(R; [1, 1]) = \begin{cases} -\tfrac{1}{4}R^{-5} & \text{for TD} \qquad (B\,19) \\ 0 & \text{for DDQ, DQQ and TQ.} \qquad (B\,20) \end{cases}$$

B. Larsen *et al.*

Table 11. Graphs which contribute to the density expansion of $I_{\text{triple}}^{\text{HS}}(x)$ for dipole–dipole–quadrupoles (DDQ) and dipole–quadrupole–quadrupoles (DQQ).

		DDQ	DQQ
J_0		139·4906	139·4906
J_1		· 67·1805	107·5747
		107·5747	83·7731
J_2	PY	− 13·6752	21·4919
	exact	− 9·9750	28·3571
	PY	21·4918	0·0271
	exact	28·3570	5·1150
		37·3829	95·0517
		66·2169	72·7141
J_3	PY	− 8·4649	− 9·2982
	exact	− 16·0032	− 16·4689
	PY	− 9·2982	− 7·9830
	exact	− 16·4689	− 15·1330
	PY	− 5·9914	30·8373
	exact	− 3·9501	37·2740
	PY	26·4065	6·3534
	exact	30·9811	10·9260
	PY	− 1·5615	21·6993
	exact	2·3418	26·4960
		45·5745	70·5216

Under DDQ, ○ represents a quadrupole and ● a dipole. The opposite holds for DQQ.

The results for TQ were obtained in I, but are included here for completeness. Using these results in (B 15), we find that

$$J_0 = \begin{cases} \dfrac{5\pi^2}{3} = 16 \cdot 4493 & \text{(TD)} & \text{(B 21)} \\[2ex] \dfrac{424\pi^2}{25} = 139 \cdot 491 & \text{(DDQ and DQQ)} & \text{(B 22)} \\[2ex] 54\pi^2 = 532 \cdot 96 & \text{(TQ)}. & \text{(B 23)} \end{cases}$$

J_0 for TD agrees with an earlier calculation by Rushbrooke, Stell and Høye [2]. In what follows, it is convenient to discuss the remaining coefficients for TD and TQ interactions separately from the DDQ and DQQ interactions, because the results for the latter were almost entirely obtained numerically.

In the case of *triple–dipoles and triple–quadrupoles*, the expressions for J_1, J_2 and J_3 are

$$J_1 = 24\pi^2 \int_1^2 II'(R; [1, 1]) g_1(R) R\, dR, \tag{B 24}$$

$$J_2 = 24\pi^2 \left[\int_1^2 II'(R; [1, 1]) g_2(R) R\, dR + \int_2^3 II(R; [1, 1]) g_2(R) R\, dR \right.$$
$$\left. + \int_1^2 II'(R; [g_1(s), 1]) g_1(R) R\, dR \right], \tag{B 25}$$

$$J_3 = 48\pi^2 \left[\int_1^2 II'(R; [g_1(s), 1]) g_2(R) R\, dR \right.$$

$$\left. + \int_2^3 II(R; [g_1(s), 1]) g_2(R) R\, dR \right]$$

$$+ 24\pi^2 \left[\int_1^2 II'(R; [1, 1]) g_3(R) R\, dR \right.$$

$$\left. + \int_2^4 II(R; [1, 1]) g_3(R) R\, dR \right]$$

$$+ 8\pi^2 \int_1^2 II'(R; [g_1(s), g_1(r)]) g_1(R) R\, dR. \tag{B 26}$$

Using (B 16) and (B 18) in (B 24), we immediately have

$$J_1 = \begin{cases} \dfrac{23\pi^3}{36} = 19 \cdot 8096 & \text{(TD)}, & \text{(B 27)} \\[2ex] \left(\dfrac{4923}{16} - 384 \ln 2\right)\pi^3 = 1287 \cdot 35 & \text{(TQ)}. & \text{(B 28)} \end{cases}$$

In (B 25) and (B 26) the terms involving $II(R; [1, 1])$ are zero for TQ according to (B 20). The various other kernels in (B 25) and (B 26) have been given earlier for TQ so we will only quote the results for TD. We find that for
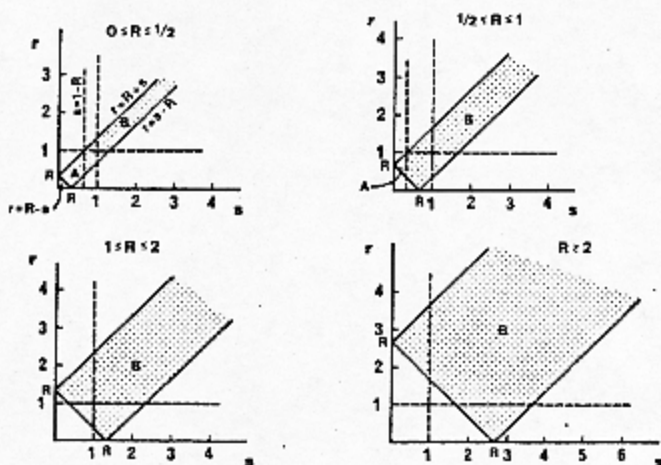
Figure 7. Integration regions of I_{TC}^{HS} with use of the superposition approximation for the three-particle correlation function h_{123}^{HS} and bi-polar coordinates (C 3).

triple–dipoles :

$$II'(R ; [g_1(s), 1]) = \pi \left[\left(-\frac{1}{576} - \frac{\ln 2}{96} \right) R + \left(\frac{5}{48} - \frac{3 \ln 2}{32} \right) R^{-1} \right. $$
$$\left. + \left(\frac{27}{128} - \frac{9 \ln 2}{32} \right) R^{-3} + \left(-\frac{311}{1152} + \frac{37 \ln 2}{96} \right) R^{-5} \right], \quad \text{(B 29)}$$

$$II(R ; [g_1(s), 1]) = \pi \left[\left(-\frac{17}{1152} - \frac{1}{96} \ln \left(\frac{2}{R-1} \right) \right) R + \frac{1}{96} \right. $$
$$+ \left(\frac{17}{384} - \frac{3}{32} \ln \left(\frac{2}{R-1} \right) \right) R^{-1} + \frac{11}{72} R^{-2} + \left(\frac{7}{384} - \frac{9}{32} \ln \left(\frac{2}{R-1} \right) \right) R^{-3}$$
$$\left. - \frac{111}{288} R^{-4} + \left(\frac{193}{128} + \frac{37}{96} \ln \left(\frac{2}{R-1} \right) \right) R^{-5} \right], \quad \text{(B 30)}$$

and

$$II'(R ; [g_1(s), g_1(r)]) = \pi^2 \left[- \left(\frac{1}{13824} + \frac{\ln 2}{1152} + \frac{(\ln 2)^2}{384} \right) R \right. $$
$$+ \left(\frac{19}{2304} + \frac{5 \ln 2}{128} - \frac{(\ln 2)^2}{16} \right) R^{-1} + \left(\frac{81}{512} - \frac{99 \ln 2}{256} + \frac{(\ln 2)^2}{4} \right) R^{-3}$$
$$\left. + \left(\frac{1163}{13824} - \frac{143 \ln 2}{1152} \right) R^{-5} \right]. \quad \text{(B 31)}$$

The analytic expression for g_1 [30] has been used in evaluating these kernels. To proceed further in the calculation of J_2 and J_3, we need the coefficients of x^2 and x^3 in the density expansion of the hard-sphere radial distribution function. The coefficient of x^2 is available analytically [32], but $g_3(\ )$ is only available

numerically as a function of the interatomic distance [31]. In the Percus–Yevick (PY) approximation, however, the cluster diagrams which contribute to $g_3(\ )$ are known in closed form [33], and one can show,

$$g_3^{\mathrm{PY}}(R) = =\pi^3\left(\frac{R^9}{453600} - \frac{R^7}{2520} + \frac{2R^6}{945} + \frac{R^5}{90} - \frac{191R^4}{1800} + \frac{77R^3}{432}\right.$$

$$\left. + \frac{443R^2}{1260} - \frac{1789R}{1440} + \frac{22843}{22680} - \frac{4433R^{-1}}{25200}\right) \qquad (1 \leqslant R \leqslant 2)$$

$$= \pi^3\left(-\frac{R^9}{226800} + \frac{R^7}{1260} - \frac{4R^6}{945} - \frac{R^5}{45} + \frac{83R^4}{360} - \frac{205R^3}{432}\right.$$

$$\left. - \frac{191R^2}{252} + \frac{1141R}{288} - \frac{20323}{4536} + \frac{29683R^{-1}}{25200}\right) \qquad (2 \leqslant R \leqslant 3)$$

$$= \pi^3\left(\frac{R^9}{453600} - \frac{R^7}{2520} + \frac{2R^6}{945} + \frac{R^5}{90} - \frac{28R^4}{225} + \frac{8R^3}{27}\right.$$

$$\left. + \frac{128R^2}{315} - \frac{128R}{45} + \frac{11264}{2835} - \frac{2048R^{-1}}{1575}\right) \qquad (3 \leqslant R \leqslant 4)$$

$$= 0 \qquad (4 \leqslant R). \quad (\mathrm{B}\ 32)$$

We have not found this expression given explicitly anywhere in the literature. Using (B 32) and the analytic expression for $g_2^{\mathrm{PY}}(R)$, we find that

(*a*) For triple–dipoles :

$$J_2^{\mathrm{PY}} = \pi^4\left[\frac{43915621}{6350400} - \frac{66961}{10080}\ln 2 + \frac{361}{48}(\ln 2)^2 - \frac{16}{3}\ln 3\right]$$

$$= 6.3321 \qquad (\mathrm{B}\ 33)$$

and

$$J_3^{\mathrm{PY}} = \pi^5\left[\frac{132783090133}{4000752000} - \frac{788788559}{25401600}\ln 2 + \frac{456805}{8064}(\ln 2)^2\right.$$

$$\left. - 2(\ln 2)^3 - \frac{4441}{240}\ln 3 - \frac{1223}{42}(\ln 2)(\ln 3) + \frac{1223G}{42}\right]$$

$$= -0.0932, \qquad (\mathrm{B}\ 34)$$

where in (B 34)

$$G = \int_2^3 R^{-1}\ln(R-1)\,dR \simeq 0.147221 \qquad (\mathrm{B}\ 35)$$

cannot be expressed in closed form,

(*b*) For triple quadrupoles,

$$J_2^{\mathrm{PY}} = \pi^4\left[\frac{50669883667}{88309760} - \frac{1552087}{1792}\ln 2 + \frac{345}{4}(\ln 2)^2\right]$$

$$= 1447.9762, \qquad (\mathrm{B}\ 36)$$

1018   B. Larsen *et al.*

and

$$J_3^{PY} = \pi^6 \left[\frac{10008765268937921}{13352435712000} - \frac{18084526909}{15052800} \ln 2 + \frac{37657}{70} (\ln 2)^2 \right.$$
$$\left. + \frac{3}{16} (\ln 2)^3 + \frac{8559}{2240} \ln 3 - \frac{20079}{70} (\ln 2)(\ln 3) + \frac{20079G}{70} \right]$$
$$= 1026 \cdot 3847. \tag{B 37}$$

The result for J_2^{PY} for TQ has been given in I, and is included here again for completeness.

The other estimates of J_2 and J_3 for TD and TQ given in table 1 have been obtained using the SA in connection with the exact $g_2(\ )$ and $g_3(\ )$ coefficients for hard spheres. The final integrations (B 25) and (B 26) were done numerically using our analytic expressions for the kernels and the tabulations of $g_2(R)$ and $g_3(R)$ given by Ree *et al.* [31]. Our analytic and numerical work on the integrals which contribute to J_2 and J_3 for TD and TQ is summarized in table 10.

For the unsymmetrical DDQ and DQQ we found it easier to determine all but the most elementary kernels of J_1, J_2 and J_3 numerically because relatively simple expressions like (B 24)–(B 26) are not obtained in these cases. We followed the numerical procedure described in Appendix D, replacing the full radial distribution functions $g(R)$, $g(s)$ and $g(r)$ by the required combinations of the coefficients in their respective density expansions. As a check on the procedure, the analytic results for TD and TQ were compared with the corresponding numerical estimates, and the numerical error was never found to be greater than 0·1 per cent. Internal consistency was also checked by evaluating

diagrams (see (B 9)–(B 11)) giving equal contributions, e.g. △ and △ ,

separately, and the inconsistency was never found to be greater than 0·1 per cent. The results for DDQ and DQQ are given in table 11.

Appendix C
Density expansion of the triple-charge integral $I_{TC}^{HS}(x)$ using the superposition approximation

We define $I_{TC}^{HS}(x)$ by (3.12) except that g_{123}^{HS} is replaced by h_{123}^{HS} and W_{triple} is now $(Rsr)^{-1}$. In bi-polar coordinates this becomes

$$I_{TC}^{HS}(x) = 8\pi^2 \int_0^\infty dR \int_0^\infty ds \int_{|R-s|}^{R+s} h_{123}^{HS}(R, s, r) \, dr. \tag{C 1}$$

Since we have h_{123}^{HS} instead of g_{123}^{HS} in the integrand, the method of integration used in Appendix B has to be slightly modified. Use of the superposition approximation [10]

$$h_{123}^{HS}(R, s, r) = h(R)h(s)h(r) + h(R)h(s) + h(R)h(r) + h(s)h(r) \tag{C 2}$$

converts (C 1) to

$$\frac{I_{TC}^{HS}(x)}{8\pi^2} = \int_0^\infty h(R) \, dR \int_0^\infty h(s) \, ds \int_{|R-s|}^{R+s} h(r) \, dr$$
$$+ 3 \int_0^\infty h(R) \, dR \int_0^\infty h(s)(R+s-|R-s|) \, ds, \tag{C 3}$$

where it is understood without further specification that the pair correlation functions $h(\ )$ are those for the hard-sphere system. It is now convenient to define (see figure 7)

$$A(R;\ [h(s), h(r)]) = \int_0^{1-R} h(s)\ ds \int_{|R-s|}^{R+s} h(r)\ dr \quad R \leqslant 1 \tag{C 4}$$

$$= 0 \qquad\qquad\qquad R \geqslant 1 \tag{C 5}$$

and

$$B(R;\ [h(s), h(r)]) = \int_{1-R}^{\infty} h(s)\ ds \int_{|R-s|}^{R+s} h(r)\ dr \quad R \leqslant 1 \tag{C 6}$$

$$= \int_0^{\infty} h(s)\ ds \int_{|R-s|}^{R+s} h(r)\ dr \quad R \geqslant 1. \tag{C 7}$$

These are somewhat similar to the functions $I(R;\ [g(s), g(r)])$, etc. which appear in Appendix B. It is also convenient to define

$$C(R;\ [h(s)]) = 2 \int_0^R h(s)\ s\, ds \tag{C 8}$$

Table 12. Functions for triple-charge integrals.

$A(R;\ [h_0(s), h_0(r)])$		$B(R;\ [h_0(s), h_0(r)])$	
$-3R^2 + 2R$	$(0 \leqslant R \leqslant \frac{1}{2})$	$\dfrac{3R^2}{2}$	$(0 \leqslant R \leqslant \frac{1}{2})$
$(1-R)^2$	$(\frac{1}{2} \leqslant R \leqslant 1)$	$-\dfrac{5R^2}{2} + 4R - 1$	$(\frac{1}{2} \leqslant R \leqslant 1)$
0	$(1 \leqslant R)$	$\dfrac{R^2}{2} - 2R + 2$	$(1 \leqslant R \leqslant 2)$
		0	$(2 \leqslant R)$

$B(R;\ [h_1(s), h_0(r)])$		$B(R;\ [h_1(s), h_1(r)])$	
$\pi\left(\dfrac{R^5}{120} - \dfrac{R^3}{3} + \dfrac{4R^2}{3} - \dfrac{89R}{48} + \dfrac{59}{80}\right)$	$(1 \leqslant R \leqslant 2)$	$\dfrac{49\pi^2}{2304}$	$(1 \leqslant R \leqslant 2)$
$-\pi\left(\dfrac{R^5}{240} - \dfrac{R^4}{48} - \dfrac{R^3}{8} + \dfrac{9R^2}{8} - \dfrac{45R}{16} + \dfrac{189}{80}\right)$	$(2 \leqslant R \leqslant 3)$		

$C(R;\ [h_0(s)])$		$C(R;\ [h_1(s)])$	
$-R^2$	$(0 \leqslant R \leqslant 1)$	$\pi\left(\dfrac{R^5}{30} - \dfrac{2R^3}{3} + \dfrac{4R^2}{3} - \dfrac{7}{10}\right)$	$(1 \leqslant R \leqslant 2)$
-1	$(1 \leqslant R)$	$\dfrac{11\pi}{30}$	$(2 \leqslant R \geqslant 3)$

$D(R;\ [h_0(s)])$		$D(R;\ [h_1(s)])$	
$2R^2 - 2R$	$(0 \leqslant R \leqslant 1)$	$\pi\left(-\dfrac{R^5}{24} + R^3 - \dfrac{8R^2}{3} + 2R\right)$	$(1 \leqslant R \leqslant 2)$
0	$(1 \leqslant R)$	0	$(2 \leqslant R)$

and

$$D(R ; [h(s)]) = 2R \int_R^\infty h(s) \, ds. \qquad (C\,9)$$

Then (C 3) can be written as

$$\frac{I_{TC}^{HS}}{8\pi^2} = \int_0^\infty [A(R ; [h(s), h(r)]) + B(R ; [h(s), h(r)])]h(R) \, dR$$

$$+ 3 \int_0^\infty [C(R ; [h(s)]) + D(R ; [h(s)])]h(R) \, dR. \qquad (C\,10)$$

The advantage of writing (C 3) as (C 10) is that in certain ranges of R, the functions $A(R ; [h(s), h(r)])$, etc. take on simple analytic expressions, or are identically zero (see table 12).

Employing the density expansion for $h(R)$,

$$h(x, R) = \exp \left[-\beta u^{HS}(R)\right][h_0(R) + x h_1(R) + x^2 h_2(R) + x^3 h_3(R) + O(x^4)] \quad (C\,11)$$

where $h_0(R) \equiv 1 - \exp[\beta u^{HS}(R)]$ and $h_n(R) \equiv g_n(R)$; $n = 1, 2$ and 3, and the corresponding expansions for $h(s)$ and $h(r)$, we get the density expansion for the *triple-charge* integral

$$I_{TC}^{HS}(x) = J_0 + x J_1 + x^2 J_2 + x^3 J_3 + O(x^4). \qquad (C\,12)$$

The coefficients in this expansion may be represented graphically as

 $\qquad (C\,13)$

 $\qquad (C\,14)$

 $\qquad (C\,15)$

 $\qquad (C\,16)$

where we have used the same symbols as in (B 4)–(B 11) of Appendix B except that the bond ——— now represents h_0. As before, we have ignored any explicit representation of the triple-charge potential and the factor $\exp(-\beta u^{HS})$. Each one of these graphs can be calculated analytically, using the exact h_0 and h_1, and the Percus–Yevick (PY) approximation for h_2 and h_3 (note that h_3 in the PY approximation is given by (B 32) of Appendix B). Since $h_0(R)$, $h_1(R)$, $h_2(R)$ and $h_3(R)$ are zero beyond $r = 1, 2, 3$ and 4, respectively, and all except $h_0(R)$ are zero for $R < 1$, it follows from (C 10) and (C 11) that

$$\frac{J_0}{8\pi^2} = \int_0^1 \{A(R ; [h_0(s), h_0(r)]) + B(R ; [h_0(s), h_0(r)])\}h_0(R) \, dR$$

$$+ 3 \int_0^1 \{C(R ; [h_0(s)]) + D(R ; [h_0(s)])\}h_0(R) \, dR, \qquad (C\,17)$$

$$\frac{J_1}{8\pi^2} = 3 \int_1^2 B(R ; [h_0(s), h_0(r)])h_1(R) \, dR + 6 \int_1^2 C(R ; [h_0(s)])h_1(R) \, dR, \quad (C\,18)$$

$$\frac{J_2}{8\pi^2} = 3 \int_1^2 B(R ; \ [h_1(s), h_0(r)])h_1(R) \, dR + 3 \int_1^3 B(R ; \ [h_0(s), h_0(r)])h_2(R) \, dR$$

$$+ 3 \int_1^2 \{C(R ; \ [h_1(s)]) + D(R ; \ [h_1(s)])\}h_1(R) \, dR$$

$$+ 6 \int_1^3 C(R ; \ [h_0(s)])h_2(R) \, dR, \quad (C\ 19)$$

$$\frac{J_3}{8\pi^2} = \int_1^2 B(R ; \ [h_1(s), h_1(r)])h_1(R) \, dR + 6 \int_1^3 B(R ; \ [h_1(s), h_0(r)])h_2(R) \, dR$$

$$+ 3 \int_1^4 B(R ; \ [h_0(s), h_0(r)])h_3(R) \, dR + 6 \int_1^3 \{C(R ; \ [h_1(s)])$$

$$+ D(R ; \ [h_1(s)])\}h_2(R) \, dR + 6 \int_1^4 C(R ; \ [h_0(s)])h_3(R) \, dR. \quad (C\ 20)$$

where all the kernels that are identically zero (see table 12) are left out. Except for the factor $8\pi^2$, the integrals in (C 17) to (C 20) correspond exactly to the graphs in (C 13) to (C 16). To calculate the functions $A(R ; \ [h_0(s), h_0(r)])$, etc., we split the range of integration over R further into the intervals $(0, \frac{1}{2})$, $(\frac{1}{2}, 1)$, $(1, 2)$ and $(2, \infty)$ (see figure 7) and make use of the exact analytic expressions for h_0 and h_1 obtaining the results given in table 12. Applying this information and the analytic expressions for h_0, h_1, h_2^{PY} and h_3^{PY} to (C 17), (C 18), (C 19) and (C 20), we find that for triple-charges

$$J_0 = 12\pi^2 = 118\cdot435, \quad (C\ 21)$$

$$J_1 = -\frac{179}{30}\pi^3 = -185\cdot004, \quad (C\ 22)$$

$$J_2^{PY} = \pi^4 \left[\frac{10356583}{1058400} - \frac{648}{35} \ln\left(\frac{3}{2}\right)\right] = 221\cdot921, \quad (C\ 23)$$

$$J_3^{PY} = \pi^5 \left[\frac{53939929627}{2794176000} + \frac{114497}{525} \ln 2 - \frac{54567}{350} \ln 3\right]$$

$$= -247\cdot075. \quad (C\ 24)$$

The expressions for the individual graphs are given in table 13.

We have also calculated J_2 and J_3 by using the exact values for h_2 and h_3 in (C 19) and (C 20). With the analytic results for the kernels, only the integration over R had to be performed numerically. The results are summarized in table 13.

APPENDIX D

Numerical calculation of the triple integral $I_{\text{triple}}^{118}(x)$ using the superposition approximation

In the numerical calculation of I_{triple}^{118} it also appears useful to split the integrations into the same regions as those described in Appendix B. This is because the long-range behaviour of the $g(r)$ is essentially given by its low

B. Larsen *et al.*

Table 13. Graphs which contribute to the density expansion of $I_{TC}^{HS}(x)$

Graph		Value		Graph		Value
I_0 [graph]		-39.4784		I_3 [graph]		7.5929
[graph]		52.6379		[graph]	PY	3.3226
					exact	2.6540
J_1 [graph]		10.6799		[graph]	PY	-0.3611
					exact	-0.9374
[graph]		-36.1739		[graph]	PY	-28.1708
					exact	-26.3573
I_2 [graph]		-12.9567		[graph]	PY	-17.4156
					exact	-12.1869
[graph]	PY	2.8212				
	exact	3.5362				
[graph]		38.0530				
[graph]	PY	23.0279				
	exact	21.2108				

——— $\equiv h_0$, – – – $\equiv h_1$, ········· $\equiv h_2$ and ⌇⌇⌇ $\equiv h_3$.

density limit to which (B 13) applies in the case of hard spheres. Thereby the problem with long range integrands $(O(r^{-3})$ in the case of triple–dipoles) is considerably reduced. We are then faced with the problem of calculating the triple integral (B 1) numerically.

Provided the triple potential W_{triple} can be written

$$W_{\text{triple}}(R, s, r) = \sum_n c_n(R, s) r^n \qquad (D\ 1)$$

(which always applies in the present case), one may tabulate

$$\text{RINT}_n(q) = \int^q h(r) r^{n+1}\, dr, \qquad (D\ 2)$$

where $h(r) \equiv g(r) - 1$, in the beginning of the programme. Whenever a kernel of the type (B 2) is needed, the corresponding table values of RINT are looked up :

$$K(g\ ;\ [g(r)]) = \sum_n c_n(R, s) \left[\frac{q^{n+2}}{n+2} + \text{RINT}_n(q) \right];\quad n \neq -2, \qquad (D\ 3)$$

and the triple integral is in effect reduced to a double integral.

The actual integration procedure employed is a Richardson extrapolation of Simpson's 1/3-rule, and will be briefly described in the following. Suppose a continuous function $f(r)$ is known at $4n+1$ equidistant points. Simpson's 1/3-rule then gives an estimate for the integral

$$I \equiv \int_a^b f(r)\,dr \tag{D 4}$$

which is

$$I \simeq S_{4n} = \frac{\Delta r}{3}\,[f(r_1) + 4f(r_2) + 2f(r_3) + \ldots + 4f(r_{4n}) + f(r_{4n+1})], \tag{D 5}$$

where $\Delta r = r_i - r_{i-1}$, $r_1 = a$ and $r_{4n+1} = b$. One may show that [34]

$$I = S_{4n} + \epsilon, \tag{D 6}$$

the correction term ϵ being given by

$$\epsilon = (b-a)\,\frac{(\Delta r)^4}{180}\,f^{(4)}(\xi), \tag{D 7}$$

where $f^{(4)}(\ )$ is the fourth derivative of $f(\ )$ and ξ some value $a \leqslant \xi \leqslant b$. If now every second point of the tabulated function is used to evaluate

$$S_{2n} = \frac{2\Delta r}{3}\,[f(r_1) + 4f(r_3) + 2f(r_5) + \ldots + 4f(r_{4n-1}) + f(r_{4n+1})], \tag{D 8}$$

we have

$$I = S_{2n} + \epsilon' ; \tag{D 9}$$

$$\epsilon' = (b-a)\,\frac{16(\Delta r)^4}{180}\,f^{(4)}(\xi') = 16\epsilon\,\frac{f^{(4)}(\xi')}{f^{(4)}(\xi)}. \tag{D 10}$$

For n sufficiently large, one may approximate $f^{(4)}(\xi') \simeq f^{(4)}(\xi)$, which yields $\epsilon' \simeq 16\epsilon$ and

$$I = S_{4n} + \epsilon \simeq S_{2n} + 16\epsilon, \tag{D 11}$$

which can be solved for I. The result is a very accurate estimate of I [35] :

$$I = (16S_{4n} - S_{2n})/15 \tag{D 12}$$

which is obtained with little extra labour compared to the ordinary Simpson's 1/3-rule. A complete description of the programme is given elsewhere [36].

Each of the kernels $I(R ; [g(s), g(r)])$, etc. of (B 1) was calculated according to their definitions and the procedure described above with $\Delta s = \Delta r = 0.05$, and tabulated at intervals $\Delta R = 0.05$. The integrals were truncated at $R = 5.9$, $s = 6.9$ and $r = 12.8$. In addition to the tests of the numerical accuracy described in Appendix B, some calculations were performed with truncations at $R = 12.3$, $s = 13.3$ and $r = 25.6$ (when PY radial distribution functions were used), and the difference in $I_{\text{triple}}^{\text{IIS}}(x)$ between the two sets of data was never found to exceed 0.05 per cent at any density. The effect of reducing the intervals to $\Delta R = \Delta s = \Delta r = 0.025$ was also examined and always found to be less than 0.05 per cent. For triple-dipoles (TD) the integrals were truncated at $R = 11.65$, $s = 12.65$ and $r = 24.3$. Since $II(R ; [1, 1])$ is non-vanishing for TD, a

B. Larsen *et al.*

Table 14. Values of $I_{triple}^{HS}(x)$ as obtained from the numerical integration with Percus–Yevick (PY) and exact (ex) hard-sphere radial distribution functions. In the case of PY, $\Delta R = \Delta s = \Delta r = 0.05$ was used, otherwise $\Delta R = \Delta s = \Delta r = 0.04$. In all ' ex ', cases, the integration was truncated at $R = s = r = 8.0$, otherwise at $R = 5.9$, $s = 6.9$ and $r = 12.8$ except for TD(PY) where truncation was made at $R = 11.65$, $s = 12.65$ and $r = 24.3$. The TD results have been corrected as described in Appendix D.

x	TD (PY)	TD (ex)	DDQ (PY)	DDQ (ex)	DQQ (PY)	DQQ (ex)	TQ (PY)	TQ (ex)
0·5	27·8282		308·667		383·830		1703·275	
0·66845	32·1470	32·3308	391·185	395·234	525·846	534·078	2465·908	2520·341
0·7	32·9639		408·204		556·836		2638·897	
0·76394	34·6159	34·8408	444·186	448·713	624·217	633·499	3022·602	3087·380
0·8	35·5423		465·346		664·997		3259·725	
0·85944	37·0547	37·2760	501·537	505·596	736·655	745·684	3685·071	3752·009
0·89763	38·0125	38·2562	525·625	530·256	785·680	796·360	3982·289	4071·641
0·9	38·0715		527·141		788·803		4001·397	
0·93583	38·9581	38·9709	550·338	550·434	837·008	839·694	4298·833	4344·752
1·0	40·5067		593·193		928·579		4877·409	

correction $8\pi^2(4/3) \int_{11\cdot65}^{\infty} dR/R^4 = 0\cdot0222$ (see (B 19)) was added to the numerical results for $I_{TD}^{HS}(x)$.

The results of the numerical calculations of $I_{triple}^{HS}(x)$ for TD, DDQ, DQQ and TQ using the PY and exact radial distribution functions for hard spheres are given in table 14. These data were used together with the density expansion of $I_{triple}^{HS}(x)$ to obtain the extended virial approximation of the triple integral which is discussed in §3.

In the case of triple-charges (TC), the superposition approximation was again assumed and the numerical calculation was based on (C 3). The problem with the discontinuity of $h(r)$ at $r=1$ was solved by defining

$$\Delta h(r) \equiv h(r) - \exp(-\beta u^{HS})h_0(r), \qquad (D\ 13)$$

where $h_0(r)$ is the coefficient of x^0 in (C 11). Introducing this into (C 3), and making use of the results listed in table 12, we get

$$\frac{I_{TC}^{HS}(x)}{8\pi^2} = \frac{J_0}{8\pi^2} + 3 \int_1^2 B(R\ ;\ [h_0(s), h_0(r)])\Delta h(R)\ dR$$

$$+ 3 \int_1^\infty B(R\ ;\ [\Delta h(s), h_0(r)])\Delta h(R)\ dR$$

$$+ 6 \int_1^\infty C(R\ ;\ [h_0(s)])\Delta h(R)\ dR + 3 \int_1^\infty \{C(R\ ;\ [\Delta h(s)])$$

$$+ D(R\ ;\ [\Delta h(s)])\}\Delta h(R)\ dR$$

$$+ \int_1^\infty \Delta h(R)\ dR \int_1^\infty \Delta h(s)\ ds \int_{\max(1,\ |R-s|)}^{R+s} \Delta h(r)\ dr. \qquad (D\ 14)$$

Table 15. Values of $I_{TC}^{HS}(x)$ as obtained from the numerical integration with Percus–Yevick (PY) and exact (ex) hard-sphere pair-correlation functions. Calculations were done with $\Delta R = \Delta s = \Delta r = 0\cdot05$ and truncation of the integral at $R=12\cdot15$, $s=13\cdot15$ and $r=25\cdot3$, and $\Delta R = \Delta s = \Delta r = 0\cdot04$ and truncation at $R=s=r=8\cdot0$ in the PY and ex cases, respectively. A Fourier transform method was applied to the PY case only, as a check.

	Bi-polar coordinates (D14)		Fourier transform method
x	PY	ex	
0·5	61·5872		61·5572
0·66845	51·8605	51·8032	51·7928
0·7	50·3970		50·3202
0·76394	47·7431	47·6156	47·6365
0·8	46·4122		46·2888
0·85944	44·6725	44·4706	44·5041
0·89763	43·6394	43·5918	43·4421
0·9	43·5765		43·3774
0·93583	43·1016	43·2271	42·8605
1·0	42·1690		41·8528

All terms of (D 14) contain only functions that are continuous in the actua
integration regions, and all but the last term are one or two-dimensional integral
that are readily calculated numerically. The last triple integral of (D 14) i
now well suited for the procedure described earlier in this Appendix, excep
that (D 3) is modified to

$$K(q \; ; \; \{\Delta h(r)\}) = (Rs)^{-1} \, \text{RINT}_{-1}(q). \qquad \text{(D 15}$$

The calculations were carried out with $\Delta R = \Delta s = \Delta r = 0.05$ and truncatior
of the integrals at $R = 12.15$, $s = 13.15$ and $r = 25.3$, and $\Delta R = \Delta s = \Delta r = 0.0$-
and truncation at $R = s = r = 8.0$ with the PY and exact hard-sphere correlatior
functions, respectively. The results are given in table 15. The results obtaine
by a Fourier transform method using the PY correlation functions are alsc
listed in table 15, and the two sets are found to agree within 1 per cent at ai
densities. The effect of reducing the truncation distances to $R = 5.75$, $s = 6.7$
and $r = 12.5$ in the PY case was also found to be less than 1 per cent.

The results of the numerical calculation of $I_{TC}^{HS}(x)$ were combined witl
the density expansion results given in table 13 to obtain an extended viria
approximation for the triple-charge integral. Our estimates of the coefficient:
J_0 to J_5 are given in table 16.

Table 16. Coefficients of the extended virial series approximation for $I_{TC}^{HS}(x)$. Label:
'PY' and 'ex' refer to the use of Percus–Yevick and exact hard-sphere pair-
correlation functions. The coefficients J_4 and J_5 were determined by a least squares
fit of the approximant to the results given in table 15.

	J_0	J_1	J_2	J_3	J_4	J_5
PY	118·435	−185·004	221·921	−247·075	212·390	−79·599
ex	118·435	−185·004	213·163	−210·560	159·336	−54·204

REFERENCES

[1] RASAIAH, J. C., LARSEN, B., and STELL, G., 1975, *J. chem. Phys.*, **63**, 722.
[2] RUSHBROOKE, G. S., STELL, G., and HOYE, J., 1973, *Molec. Phys.*, **26**, 1199.
[3] STELL, G., RASAIAH, J. C., and NARANG, H., 1974, *Molec. Phys.*, **27**, 1393.
[4] Monte Carlo results for dipolar systems are given in PATEY, G. N., and VALLEAU, J. P.,
1973, *Chem. Phys. Lett.*, **21**, 297 ; 1974, *J. chem. Phys.*, **61**, 534. McDONALD, I.,
1974, *J. Phys. C*, **7**, 1225. VERLET, L., and WEIS, J. J., 1974, *Molec. Phys.*, **28**, 665.
The work of Patey and Valleau cited in our reference [19] extends their study to
include quadrupolar terms as well.
[5] SANDLER, S., 1974, *Molec. Phys.*, **28**, 1207.
[6] WEIS, J. J., and LEVESQUE, D., 1976, *Phys. Rev. A*, **13**, 450.
[7] SULLIVAN, D. E., DEUTCH, J. M., and STELL, G., 1974, *Molec. Phys.*, **28**, 1359.
[8] CHAMBERS, M. V., and McDONALD, I. R., 1975, *Molec. Phys.*, **29**, 1053.
[9] BARKER, J. A., 1953, *Proc. R. Soc. A*, **219**, 367.
[10] STELL, G., and LEBOWITZ, J. L., 1968, *J. chem. Phys.*, **49**, 3706.
[11] ANDERSEN, H. C., and CHANDLER, D., 1970, *J. chem. Phys.*, **53**, 547.
[12] STELL, G., and WU, K. C., 1975, *J. chem. Phys.*, **63**, 491.
[13] MAYER, J. E., 1950, *J. chem. Phys.*, **28**, 1426. FRIEDMAN, H. L., 1962, *Ionic Solution
Theory* (Interscience).
[14] STELL, G., WU, K. C., and LARSEN, B., 1976, *Phys. Rev. Lett.*, **37**, 1369.

[15] BELL, R. J., 1970, *J. Phys.* B, **3**, 751.

[16] FOWLER, R., and GRABEN, H. W., 1972, *J. chem. Phys.*, **56**, 1917.

[17] SINANOĞLU, O., 1967, *Adv. chem. Phys.*, **12**, 283.

[18] COPELAND, D. A., and KESTNER, N. R., 1968, *J. chem. Phys.*, **49**, 5214.

[19] FLYTZANI-STEPHAOPOULOS, M., GUBBINS, K. E., and GRAY, C. G., 1975, *Molec. Phys.*, **30**, 1649. PATEY, G. N., and VALLEAU, J. P., 1976, *J. chem. Phys.*, **64**, 170.

[20] RASAIAH, J. C., and STELL, G., 1974, *Chem. Phys. Lett.*, **25**, 519.

[21] BARKER, J. A., HENDERSON, D., and SMITH, W. R., 1969, *Molec. Phys.*, **17**, 579.

[22] CARNAHAN, N. F., and STARLING, K. E., 1969, *J. chem. Phys.*, **51**, 635.

[23] WAISMAN, E., and LEBOWITZ, J. L., 1972, *J. chem. Phys.*, **56**, 3093.

[24] RASAIAH, J., and STELL, G., 1970, *Molec. Phys.*, **18**, 249.

[25] ONSAGER, L., 1939, *J. phys. Chem.*, **43**, 189.

[26] RASAIAH, J. C., CARD, D. N., and VALLEAU, J. P., 1972, *J. chem. Phys.*, **56**, 248.

[27] ANDERSEN, H. C., CHANDLER, D., and WEEKS, J. D., 1972, *J. chem. Phys.*, **57**, 2626.

[28] RASAIAH, J. C., 1972, *J. chem. Phys.*, **56**, 3071.

[29] DE BOER, J., 1949, *Rep. Prog. Phys.*, **12**, 305.

[30] KIRKWOOD, J. G., 1935, *J. chem. Phys.*, **3**, 300.

[31] REE, F. H., KEELER, R. N., and McCARTHY, S. L., 1966, *J. chem. Phys.*, **44**, 3407.

[32] NIJBOER, B. R. A., and VAN HOVE, L., 1952, *Phys. Rev.*, **85**, 777.

[33] LEE, Y. T., REE, F. H., and REE, T., 1971, *Adv. chem. Phys.*, **21**, 393. There are typographical errors in some of the cluster integrals which contribute to $g_3(r)$ in this paper (corrections available from Frances Ree).

[34] See e.g., BEREZIN, I. S., and ZHIDKOV, N. P., 1965, *Computing Methods*, Vol. 1 (Pergamon Press).

[35] AMBLE, O., 1967, Lecture notes in numerical methods, Institute of Applied Mathematics, University of Trondheim-NTH.

[36] LARSEN, B., 1974, TRIPLE, a computer programme for calculating three-body integrals in statistical mechanics, Report No. 1, Department of Chemistry, University of Bergen, November.